Turbulence and Statistical Theory

Eun-jin Kim

Professor of Applied Mathematics and Physics
Fluid & Complex Systems Research Centre, Coventry University, UK

ejk92122@gmail.com
https://pureportal.coventry.ac.uk/en/persons/e-j-kim/publications/

ICTP, Trieste, 14 May, 2026

Lecture roadmap:

- **I. Fusion turbulence and statistical description** — Transport, 2nd and higher moments and closure problem, structure-based theory, spectral analysis
- **II. Information theory** — Entropy, Mutual information, transfer entropy
- **III. Information Geometry** — Information length, information rate, causal information rate
- **IV. Information Geometry of the L-H transition** — Stochastic prey-predator model vs experimental data analysis of L-H transition
- **V. Summary & Open problems**

Guiding question: which statistical descriptions retain the physics that averages and spectra throw away?

Part I - Fusion turbulence and statistical descriptions

1. Turbulent transport
   Quasi-linear / diffusive closure
   Reynolds stress
   (modified Hasegawa Wakatani model)
2. Higher moments and closure problem
3. Spectral analysis
4. Nonequilibrium tokamak turbulence

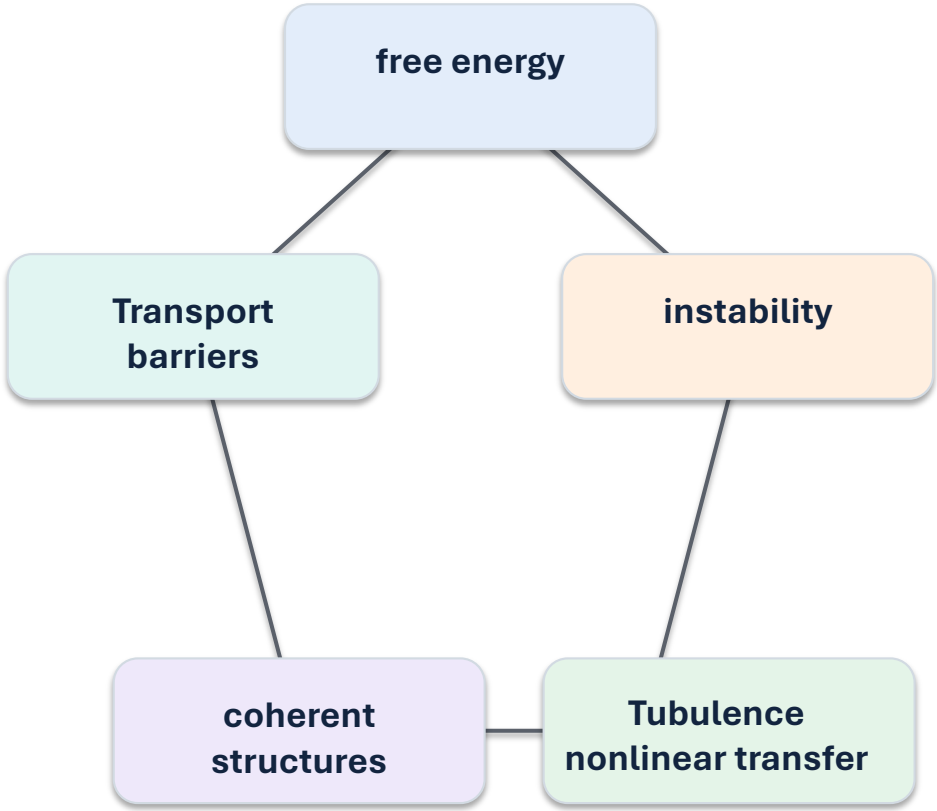

1. Quasilinear / diffusive closure

Free energy: gradients in n, T_e, T_i, p and j drive microinstabilities such as ITG, TEM, ETG, MTM, and KBM.

These generate **turbulent fluctuations**: $\tilde{n}, \tilde{p}, \tilde{\phi}, \tilde{v}_r \simeq -\frac{1}{B}\frac{\partial \tilde{\phi}}{\partial y}$

Fluxes require correlations

$$\Gamma_n = \langle \tilde{n}\, \tilde{v}_r \rangle, \qquad q = \langle \tilde{p} \tilde{v}_r \rangle$$

Quasilinear / diffusive closure gives a useful baseline

$$\mathrm{q} \simeq -\, n\, \chi_{\mathrm{eff}} \nabla < \mathrm{T} >$$

Particle transport: $\Gamma_n \simeq -D_{\mathrm{eff}} \nabla < \mathrm{n} >$

Effective coefficients give useful baseline, but they hide nonlinear and nonlocal turbulence physics

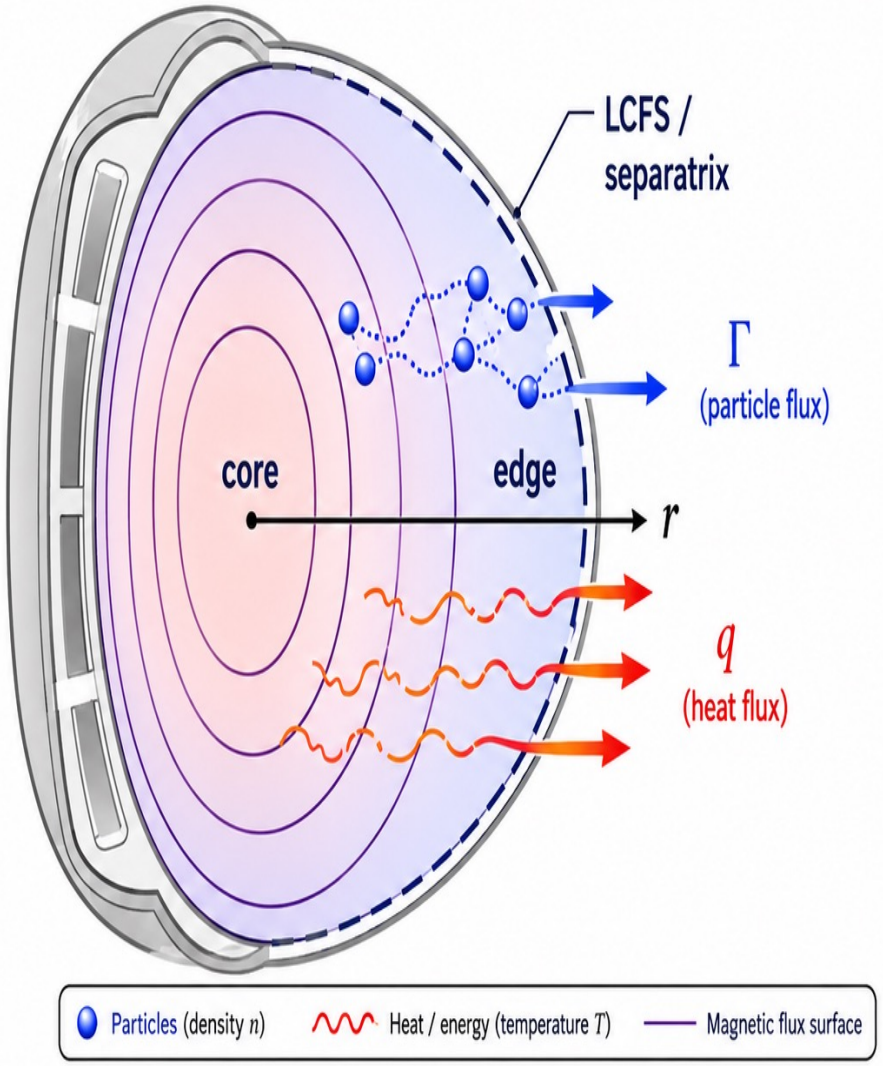

$\Gamma > 0$ and $q > 0$ indicate **outward** transport (from core toward edge).

Mini-exercise: identical mean, different risk

Use PDFs to reason about intermittent transport

Two discharges have the same mean **heat flux q.** Red discharge has a fatter positive tail in P(q) than blue one.

- Which discharge is more risky for transient wall or edge loads?

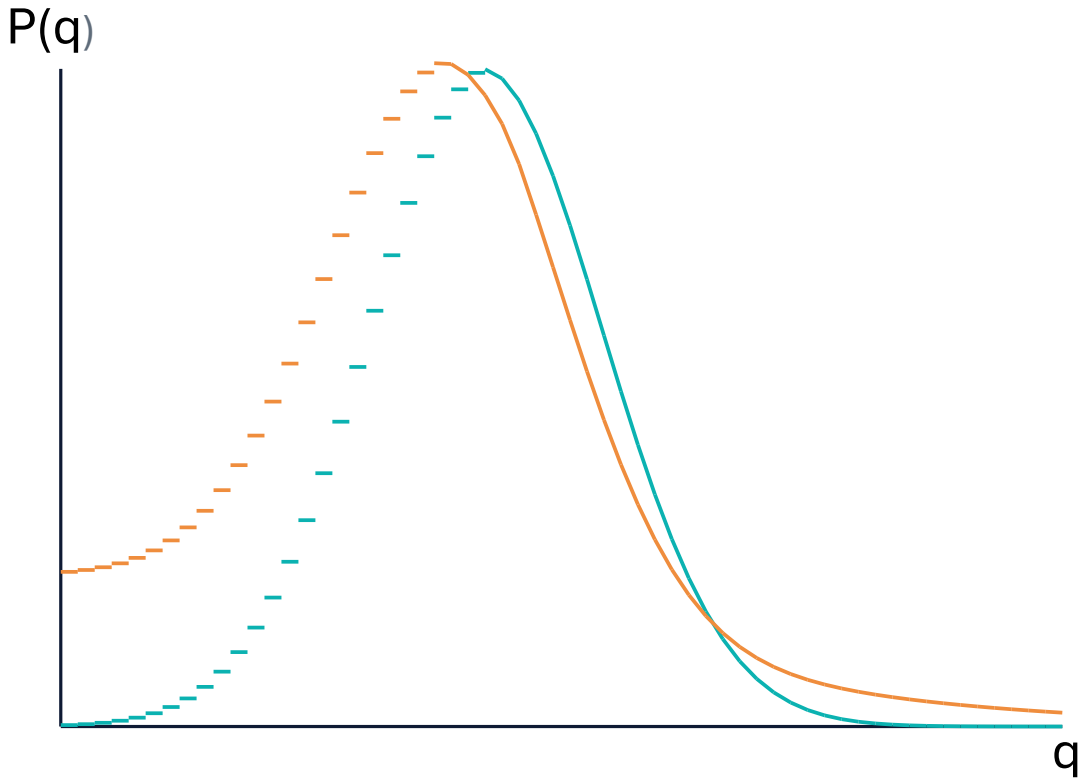

Momentum transport and zonal flow generation in fusion plasma

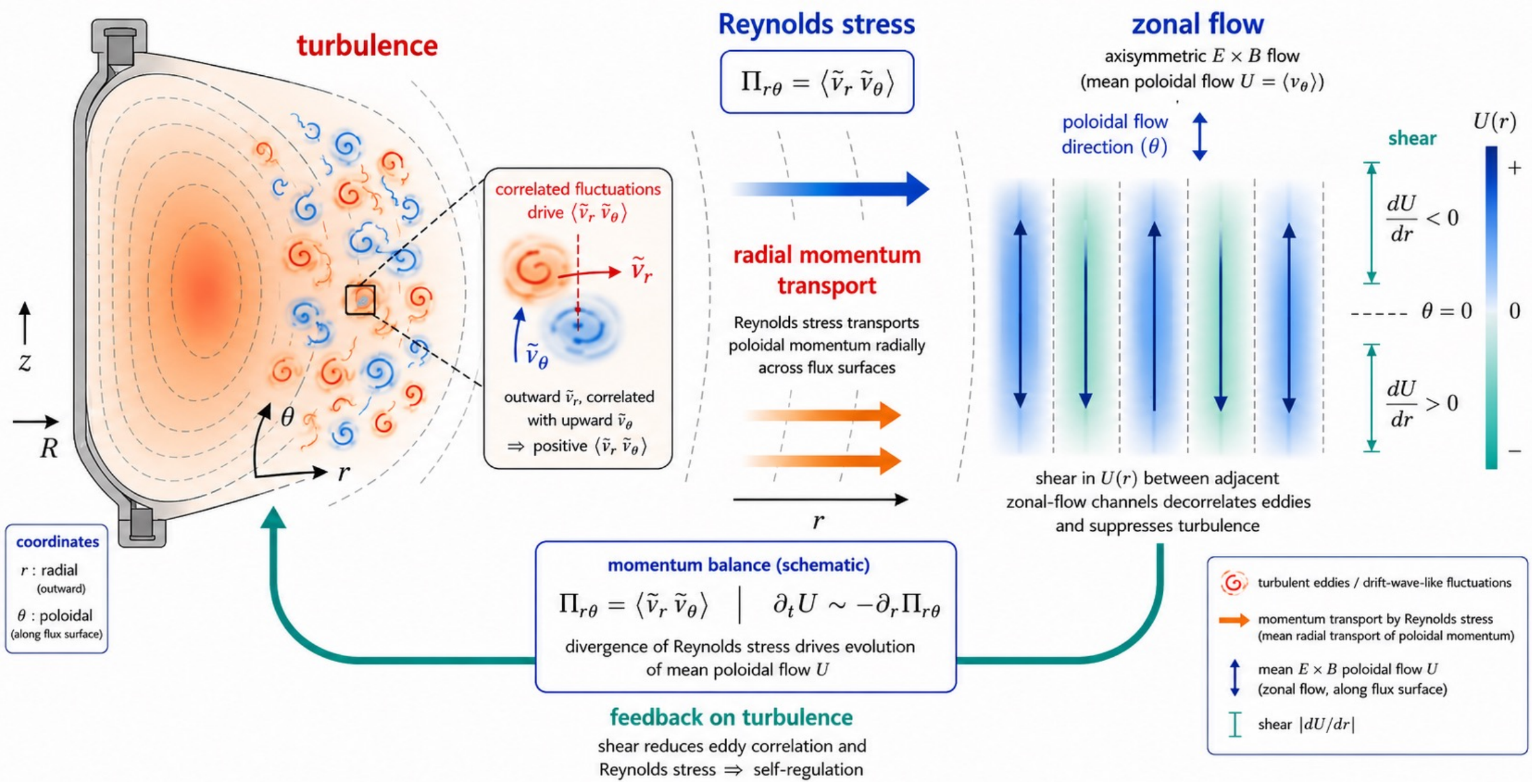

Details on quasi-linear closure for the Reynolds stress

Decompose the velocity $u_i = U_i + v_i$, use local cartesian coordinates $r = x, \theta = y$ (U_y: ZF)

- $U_i = \langle u_i \rangle = U_y$ is the mean (average) component;
- v_i is fluctuation with zero mean $\langle v_i \rangle = 0$

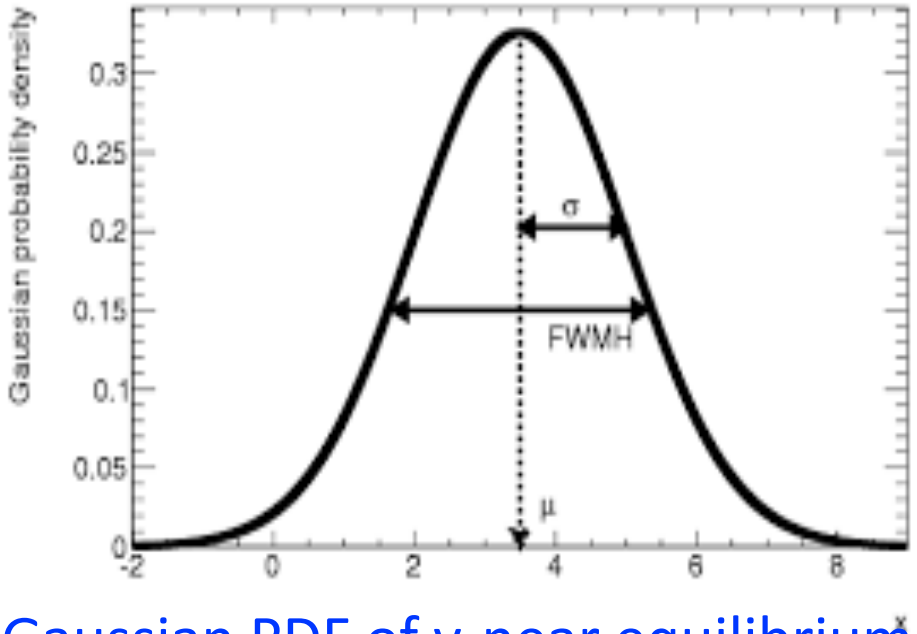

Gaussian PDF of v_i near equilibrium

U_i = μ (mean value
= PDF peak position
= most likely value)

σ: uncertainty in μ
$\langle v^2 \rangle = \sigma^2$(variance)

$$\partial_t U_y \overset{?}{=} \cdots (\nu + \nu_T)\partial_{xx} U_y$$

Reynold stress

$$\langle v_x v_y \rangle \overset{?}{=} -\nu_T \partial_x U_y$$

ν_T: turbulent viscosity (overall effects of small scales)

Modified Hasagawa-Wakatani model

[B Hnat, P Fuller, E Kim & R Hollerbach (PPCF 2025)]

Plasma density n and electrostatic potential φ, with a fixed background density gradient $n_0(x)$ and parallel electron resistivity η.

$$\frac{\partial n}{\partial t} = -\kappa\frac{\partial \phi}{\partial y} + A(\tilde{\phi} - \tilde{n}) + [n, \phi] + D\nabla^2 n,$$

$$\frac{\partial}{\partial t}\nabla^2\phi = A(\tilde{\phi} - \tilde{n}) + [\nabla^2\phi, \phi] + \mu\nabla^2(\nabla^2\phi)$$

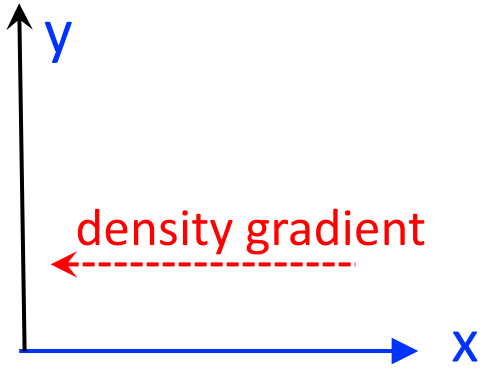

x, y: local radial, poloidal directions

$$n \to \frac{n}{n_0},\ \frac{e\phi}{T_e} \to \phi,\ L_n = \frac{[\partial_x n]}{n},\ \kappa = \frac{\rho_s}{L_n}, A = \frac{T_e k_\parallel^2}{n_0 e^2 \eta \omega_{ci}} k_\parallel^2$$

$$\omega_{ci} t \to t, \quad \rho_s(x, y) \to (x, y), \quad \langle f \rangle = \frac{1}{L_y}\int_0^{L_y} f\, dy, \quad f = \langle f \rangle + \tilde{f}$$

Here <f> is the zonal part.

- **Statistical analysis by sampling over space (zonal parts = poloidal average)**

  [A → 0: Hydrodynamic, A → ∞: Charney-Hasegawa-Mima equation]

Profiles show the formation of zonal flows over time

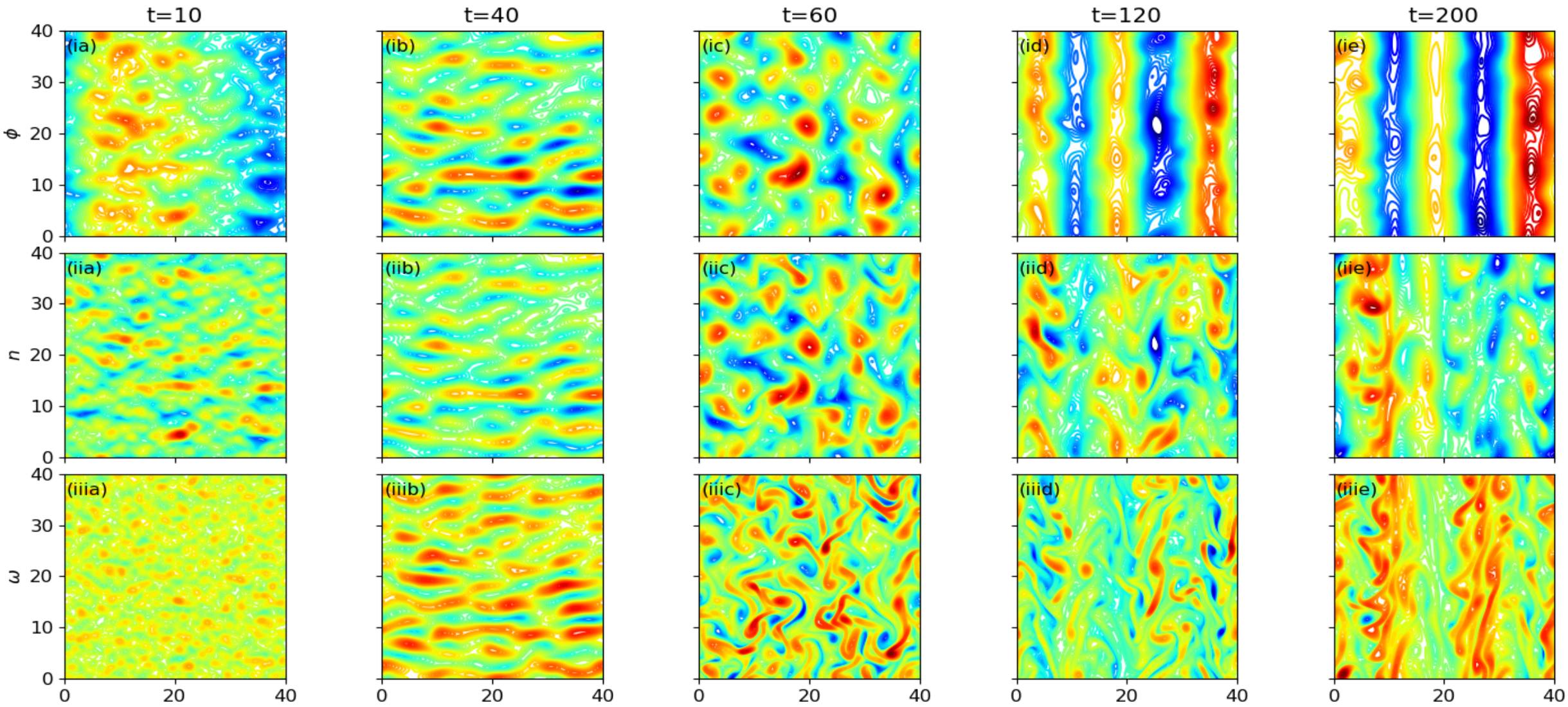

Snapshots of potential (ia)-(ie), density (iia)-(iie) and vorticity (iiia)-(iiie) at times t.

Zonal profiles reveal corrugated staircase-like structure

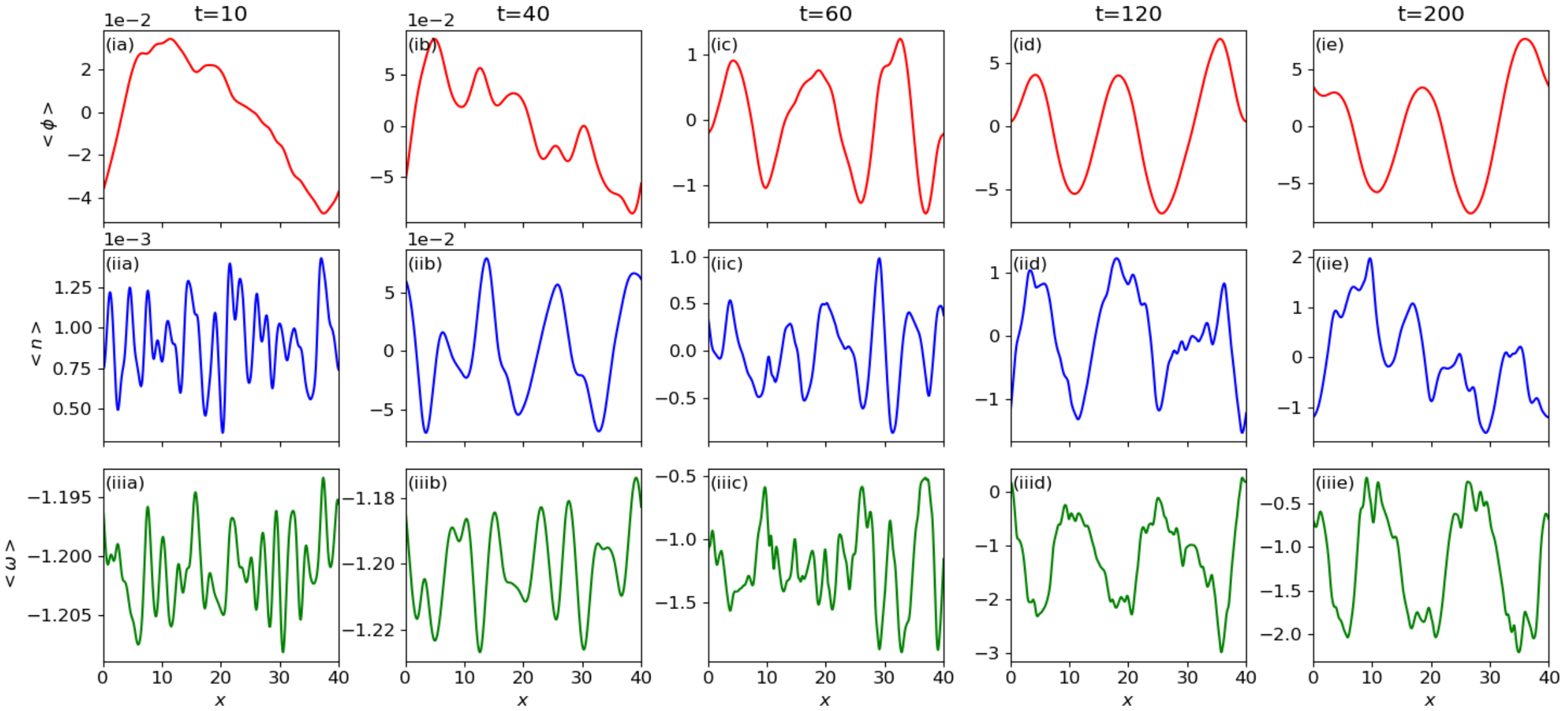

Snapshots of zonal potential (ia)-(ie), zonal density (iia)-(iie) and zonal vorticity (iiia)-(iiie)

$\langle v_x\, v_y \rangle = -\nu_T \partial_x U_y$ does not hold for constant ν_T

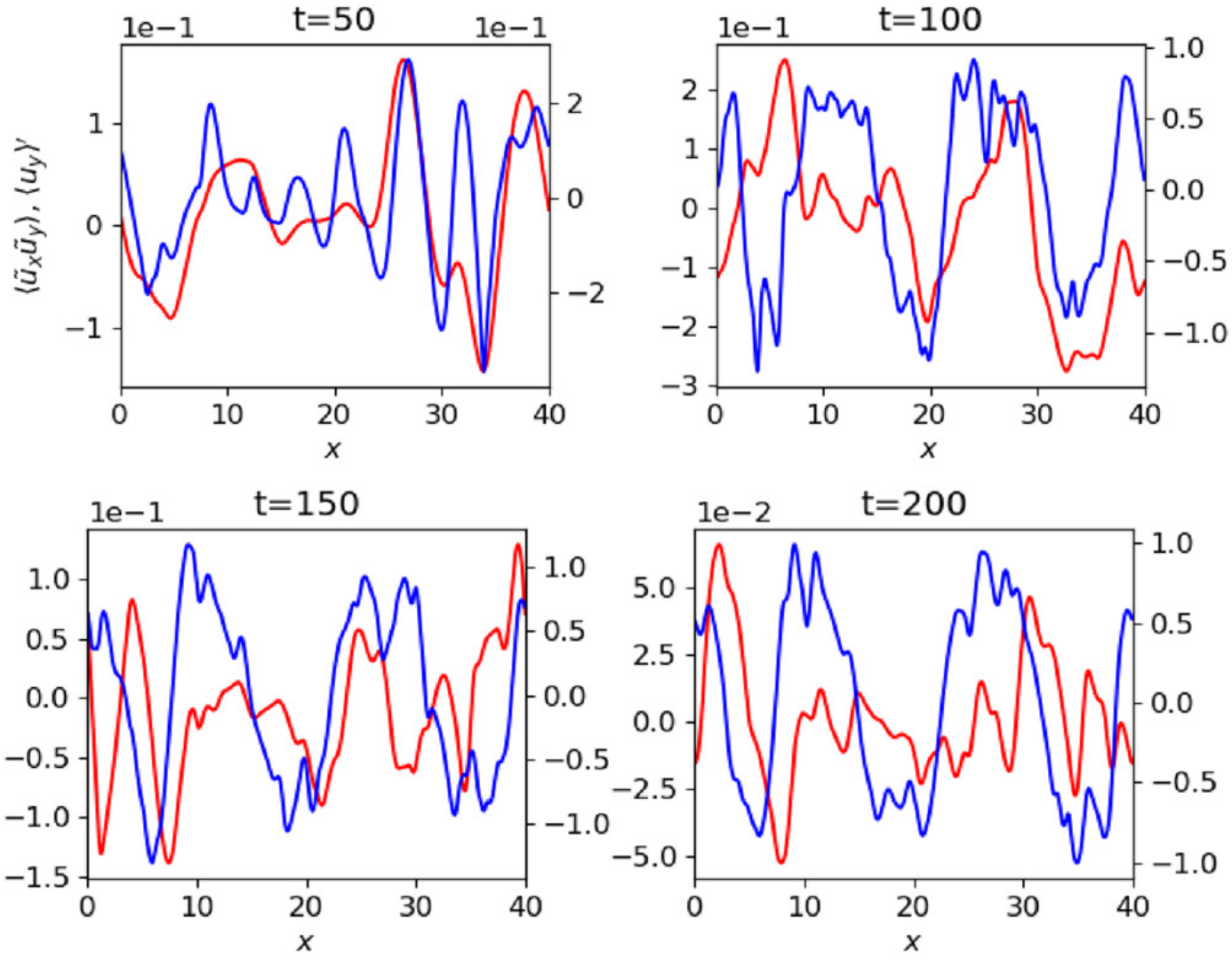

Reynolds stress $\langle v_x\, v_y \rangle$ vs $\partial_x U_y$ in blue [B Hnat, P Fuller, E Kim et al PPCF 2025]

x

PDFs of zonal parts are strongly non-Gaussian

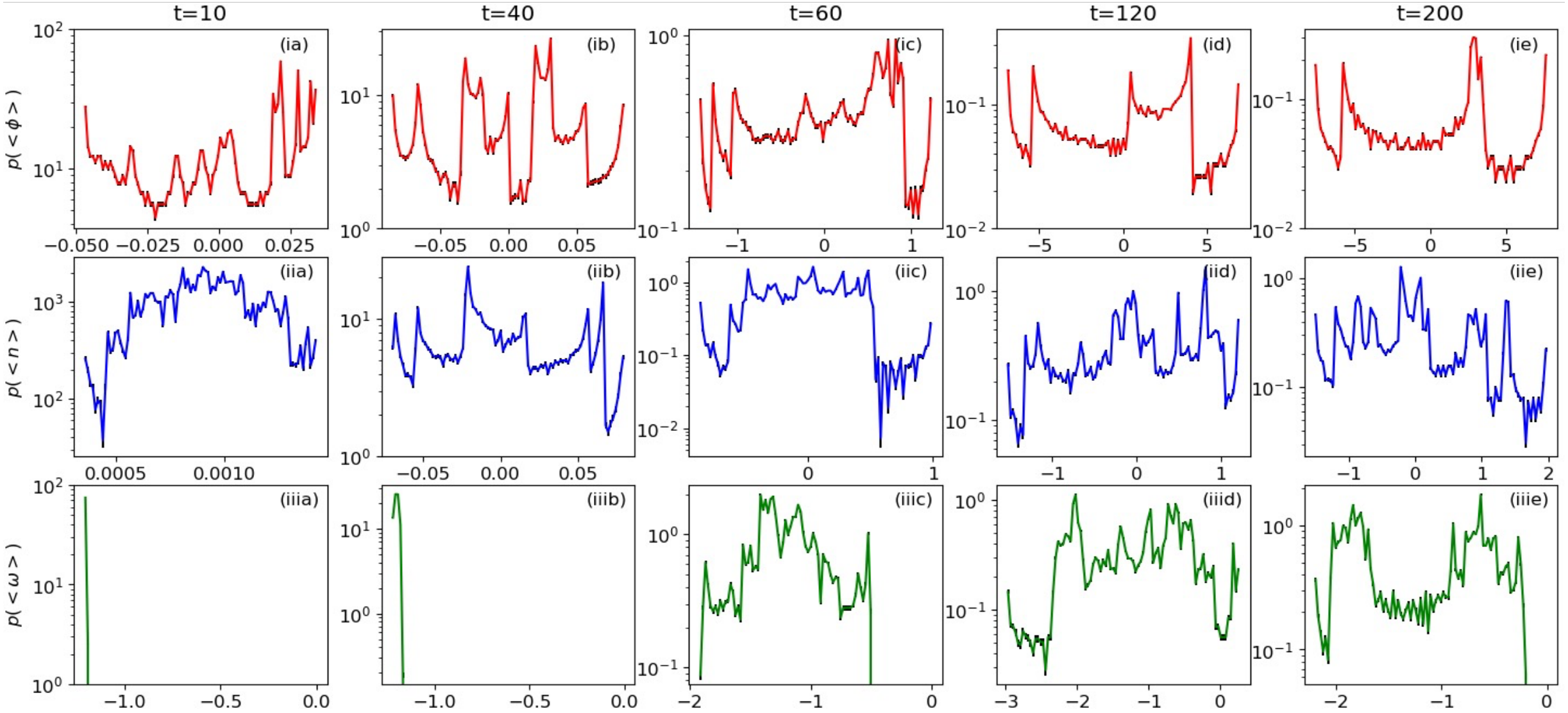

PDFs of zonal potential (ia)-(ie), zonal density (iia)-(iie) and zonal vorticity (iiia)-(iiie)

2. Higher moments and the closure problem

- Low-order moments give useful summaries: $\langle f \rangle, \langle \tilde{n}\tilde{v}_r \rangle, \langle \tilde{v}_r \tilde{v}_\theta \rangle$
- But turbulence is not fully described by averages
- Higher moments capture:
- Variance: fluctuation intensity
- Skewness: asymmetry / bursts
- Kurtosis: rare events / intermittency

Closure problem

$$\frac{d}{dt}\langle f \rangle \textit{ depends on } \langle \tilde{f}\tilde{v} \rangle$$

$$\frac{d}{dt}\langle \tilde{f}\tilde{v} \rangle \textit{ depends on higher moments}$$

To build reduced models, we must close the hierarchy.

Closures decide what turbulence physics is retained — and what is hidden.

Refs: Krommes, Phys. Rep. 360, 1 (2002); McComb, The Physics of Fluid Turbulence; Diamond et al., PPCF 47, R35 (2005).

Linear/perturbative approach is limited

- Transport coefficients: nonlocal functions of variables
- No simple flux-gradient relation due to nonlinear feedback
- Strong fluctuations, finite memory, non-Gaussian PDFs
- Non-local transport, non-diffusive transport, avalanches, blobs, streamers, nonlinear coupling of modes (J Drake 1988, W Horton 1999, P Beyer 2000, G Antar 2021, PA Politzer 2002, Dif-Pradalier 2010; 2022, X Garbet 1994, BA Cararees 1996)

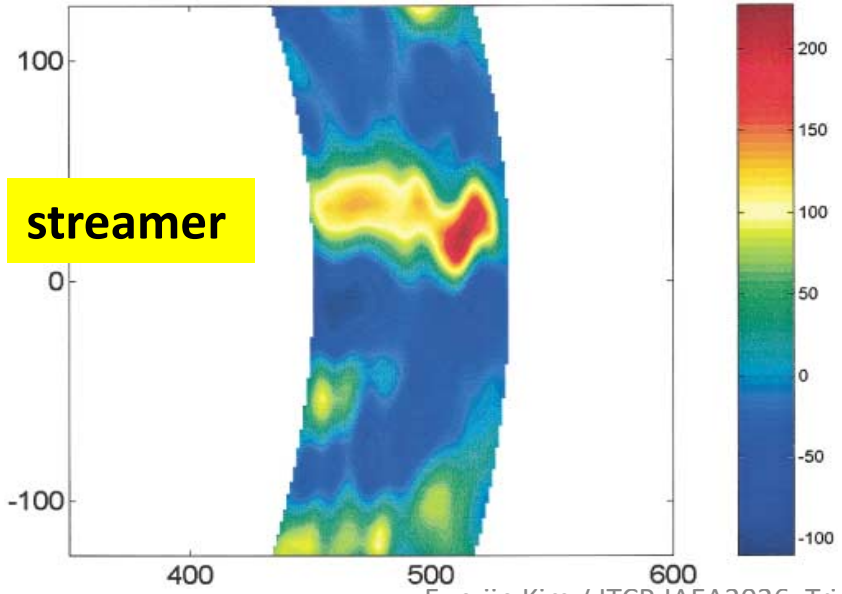

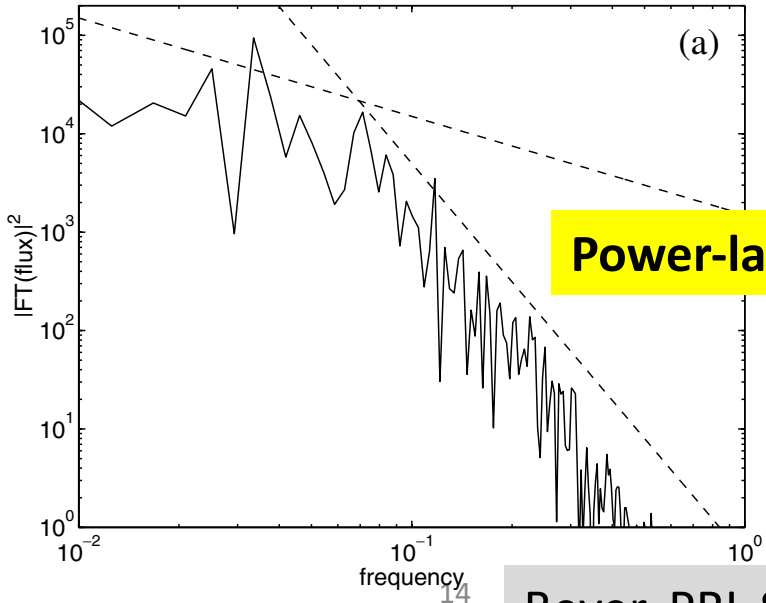

Power-law scaling

Beyer, PRL 85, 4892, 2000

Structure used for prediction of anomalous transport PDF

Stationary PDF tails for rare, large amplitude events: Instanton methods by using coherent structure as `empirical eigenfunction' ("structure-based theory) (E Kim 2002;2003;2008, J Anderson & E Kim 2008;2009)

Coherent structure

$$\phi(x,y,t) = \psi(x,y-Ut)\,F(t)$$

$$\begin{aligned}
\psi(x,y-Ut) &= c_1 J_1(kr)(\cos\theta + \epsilon\sin\theta) + \frac{\alpha}{k^2} r\cos\theta \text{ for } r \le a, \\
\psi(x,y-Ut) &= c_2 K_1(pr)(\cos\theta + \bar{\epsilon}(r)\sin\theta) \text{ for } r \ge a.
\end{aligned}$$

PDF of flux becomes a functional of F(t), PDF tail to be found by extremizing effective action S_λ

$$\begin{aligned}
P(Z) &= \langle \delta(Z_j - Z)\rangle \\
&= \int d\lambda_j \exp(i\lambda_j Z)\langle \exp(-i\lambda_j Z_j)\rangle \\
&= \int d\lambda_j \exp(i\lambda_j Z) I_{\lambda_j},
\end{aligned}$$

$$I_{\lambda_j} = \int \mathcal{D}\phi\mathcal{D}\bar{\phi}\mathcal{D}\phi_{ZF}\mathcal{D}\bar{\phi}_{ZF} e^{-S_{\lambda_j}}$$

effective action

3. Spectral view of turbulence: where does fluctuation power live?

Spectra separate turbulence by scale

$$\phi(\mathrm{x},\mathrm{t}) = \sum_k \phi_k\,(t) e^{ikx}$$

$E(k)$: spatial scales, $E(k) \propto |\,\phi_k\,|^2$

$P(\omega)$: temporal scales, $P(\omega) \propto |\,\hat{\phi}(\omega)\,|^2$

Peaks: coherent modes or characteristic frequencies (orange)
Broadband power: turbulent cascade / multiscale fluctuations (blue dashed)
Quasi-coherent mode with finite-width Peak (blue)

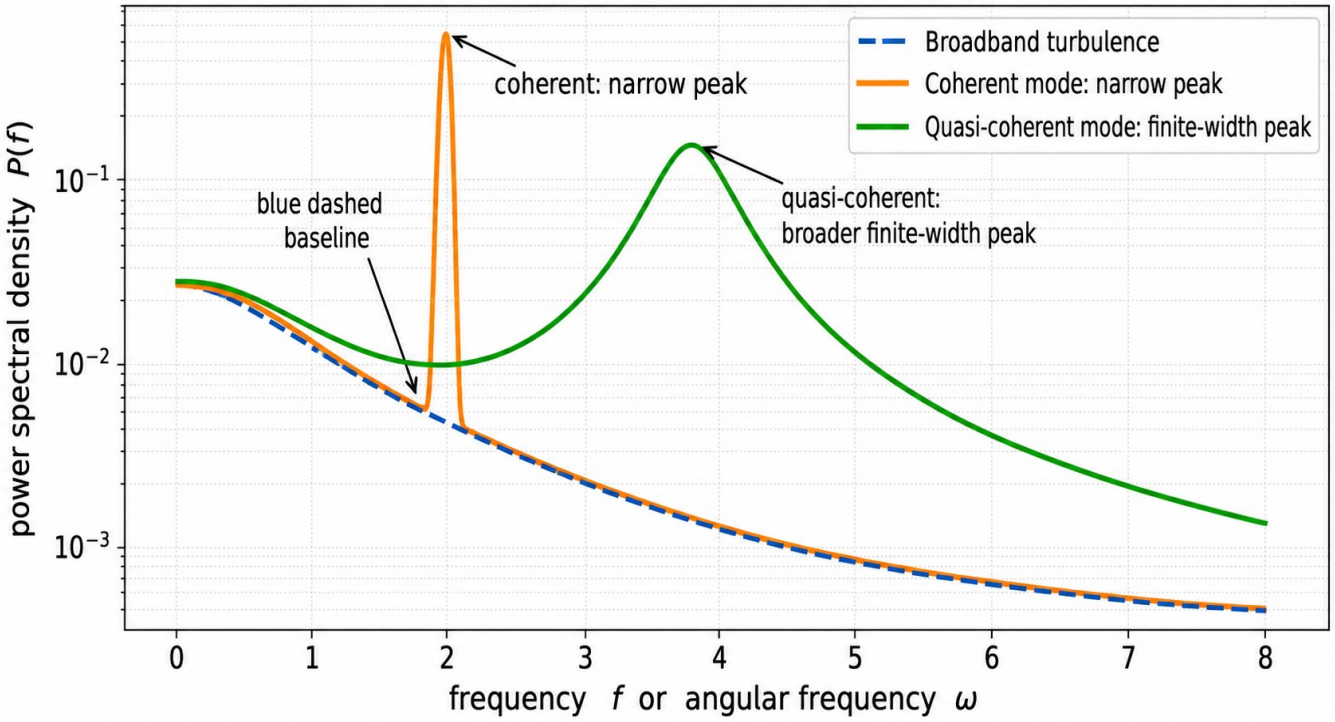

Spectra show where turbulence lives in scale space.

What can spectra tell us?

- Dominant scales: Ion-scale, electron-scale, or mixed-scale activity
- Broadband vs coherent activity: Broadband continuum suggests turbulence; narrow peaks suggest coherent or quasi-coherent modes (left figure)
- Changes across transitions: L–H transition or pedestal formation can reorganize fluctuation power across k and ω (right figure: weakly coherent mode from L mode -> I mode)
- A spectrum alone does not determine transport.
- Use spectra together with fluxes, cross-phases, PDFs, and mode fingerprints (D Hatch)

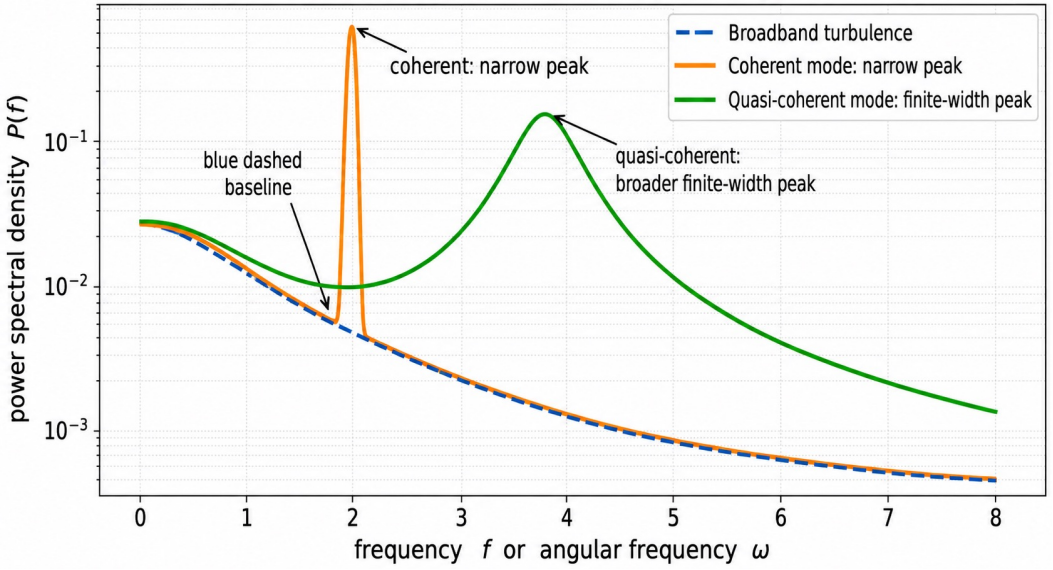

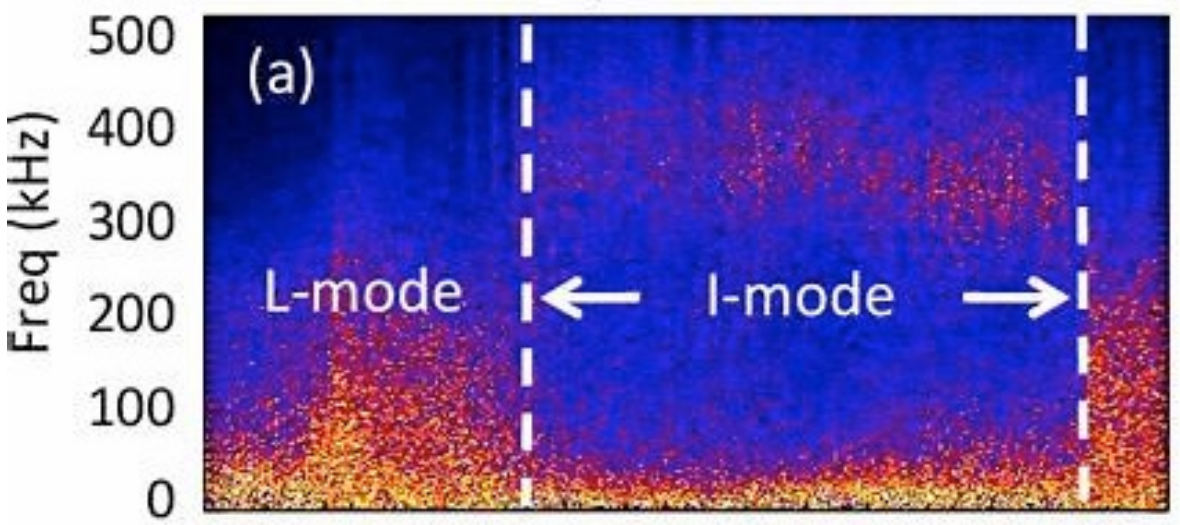

R. Bielajew et al PoP 2022, ASDEX-U

4. Non-equilibrium tokamak fusion plasmas

- Driven and/or perturbed externally with injection of heat and particles, magnetic fields and constrained by magnetic geometry
- Open boundaries and many degrees of freedom (Razumova & Lysenko, Plasma *6*, 408, 2023)
- There might be no clear timescale separation: breakdown of $\tau_G \gg \tau_M \gg \tau_F$ (timescales for global parameters, mean values, fluctuations, respectively)
- Breakdown of thermodynamic law: entropy can decrease locally with time (cf.: entropy cannot decrease with time in thermal equilibrium)
- "Non-equilibrium distance" from the Maxwellian distribution: Stix parameter $\xi = \frac{\langle P \rangle}{3nT}\tau_S$ where $\langle P \rangle \; and \; \tau_S$ are the mean absorption power and slowing-down time (K Itoh & S-I Itoh, Plasma & fusion research 10, 3401027, 2015)
- A good statistical theory must account for both typical fluctuations and rare events

Part II - Information theory

What each measure tells you

- **Entropy** H(X): uncertainty or spread of states: tracks PDF spread but may increase or decrease depending on dynamics and coordinates
- **Mutual information** I(X;Y): nonlinear dependence beyond correlation

  (I(X;Y)=0 if p(x,y)=p(x)p(y))
- Conditional mutual information I(X;Y|Z): dependence after accounting for Z
- **Transfer entropy $T_{X->Y}$** tells whether the past of X improves prediction of future Y beyond the past of Y

$$H(X) = -\sum_{x} p(x) \log p(x)$$

$$I(X;Y) = \sum_{x,y} p(x,y) \log \left[\frac{p(x,y)}{p(x)p(y)}\right]$$

Use distributions, not only trajectories.

Mutual information: nonlinear correlation detector

Why MI matters

- Linear correlation can vanish for nonlinear dependence.
- Correlation analysis is lag-dependent;
- Lagged correlation can reveal delayed linear dependence, but not general nonlinear dependence
- Mutual information detects general statistical dependence if enough data are available
- Conditional mutual information helps separate direct dependence from common-driver effects

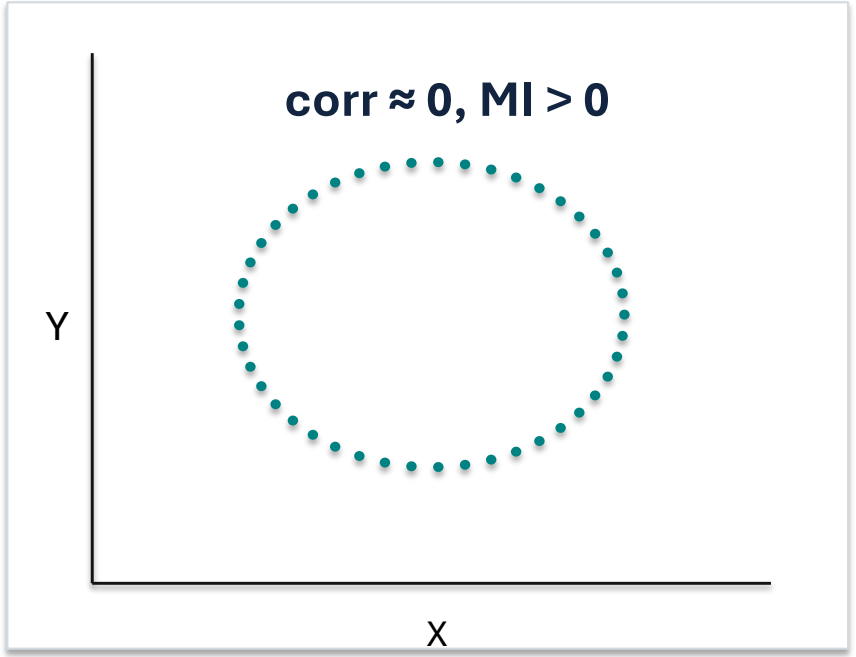

$$x = \sin(t), y = \cos(t + a)$$

$$when\ a = 0$$

$$< xy > = < sin2t > /2 = 0$$

$$\text{-> } \rho_{xy} = \frac{\langle x(t)y(t)\rangle}{\sqrt{\langle x^2(t)\rangle\langle y^2(t)\rangle}} = 0$$

Transfer entropy: van Milligen et al., Nucl. Fusion 58, 076002 (2018)

The left panel shows transfer entropy, and the right panel shows ordinary correlation, both plotted as functions of radial position and time lag in the W7-X stellarator

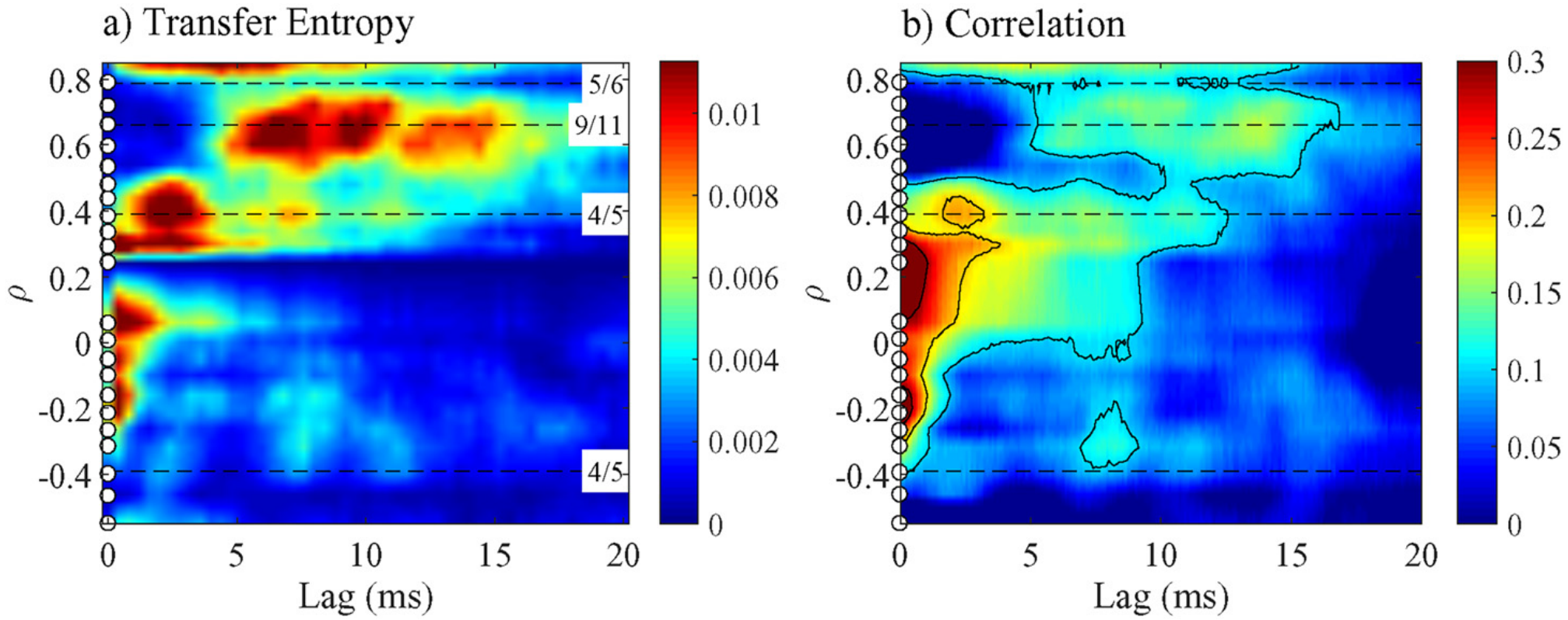

Transfer entropy identifies the rational surfaces, shown by the dashed horizontal lines, more clearly than the linear cross-correlation.

Part III - Information geometry: information length, information rate

Treat PDFs as trajectories through probability space.

Information geometry

- Application of differential geometry to probability/statistics

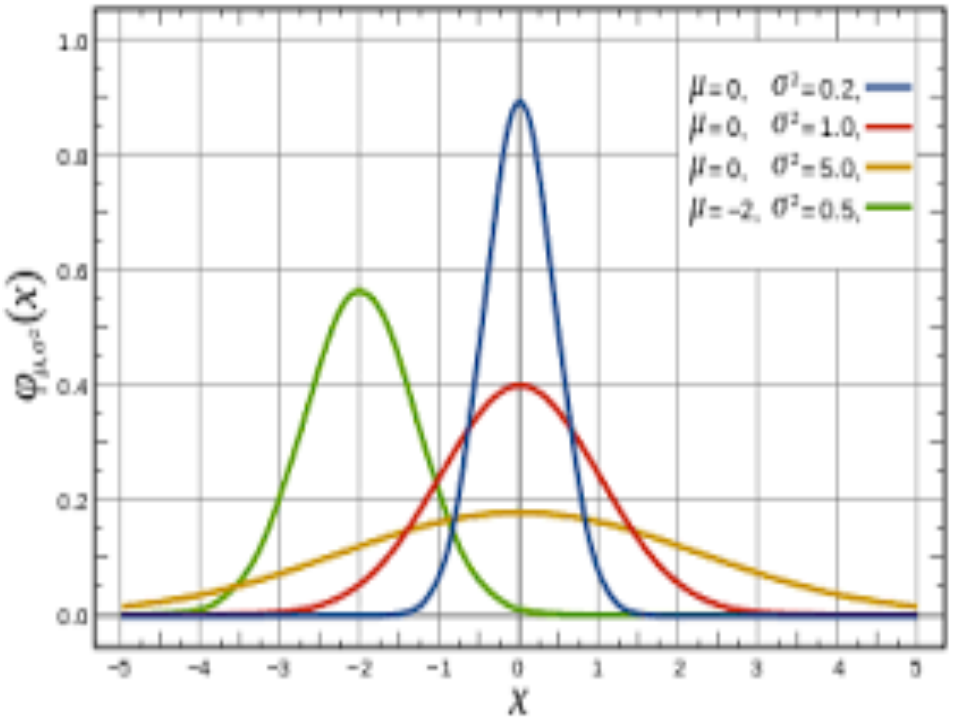

Assigning distance
Using symmetric relative entropy
(K-L divergence)

$$D(p,q) = (D_{\mathrm{KL}}(p \parallel q) + D_{\mathrm{KL}}(\mathrm{q} \parallel p))/2$$

$$D_{\mathrm{KL}}(p \parallel q) = \sum_{x} p\,(x) \log \left[\frac{p(x)}{q(x)}\right]$$

Distance measures similarity/disparity among PDFs
by dimensionless number
Smaller distance for similar PDFs
Larger distance for disparate PDFs

Infinitesimal D_{KL}

For two distributions with small difference in parameters λ and λ +d λ, the KL divergence becomes a quadratic distance-like object:

$$D_{\mathrm{KL}}\left[p(\mathrm{A} \mid \lambda) \;||\; p(\mathrm{A} \mid \lambda + d\lambda)\right] \approx \frac{1}{2} g_{ij} d\lambda_i d\lambda_j.$$

Here

$$g_{ij} = \int p\,(x \mid \lambda) \frac{\partial \ln p}{\partial \lambda_i} \frac{\partial \ln p}{\partial \lambda_j}\, dA$$

When $\lambda = t, D_{\mathrm{KL}} = \frac{1}{2}\, \Gamma^2\, (dt)^2$ where Γ denotes the information rate

$$\Gamma^2(A,t) = \int d\mathrm{A}\, p(A,t) \left(\frac{\partial \ln[p(A,t)]}{\partial t}\right)^2$$

Information rate, information length

For a time-dependent PDF p(A,t) for variable A(t) at time t $\left(\int dA\, p(A,t) = 1\right)$

$$\Gamma^2(A,t) = \mathcal{E}(A,t) = \int dA\, p(A,t)\left(\frac{\partial \ln[p(A,t)]}{\partial t}\right)^2, \qquad L(t) = \int_0^t dt_1 \Gamma(t_1)$$

- $\Gamma(A,t)$ information rate: how quickly a PDF changes (dimension [time]$^{-1}$): decorrelation rate
- $L(A,t)$ information length: cumulative change in p(A,t), the total number of different statistical states (dimensionless "distance", ΔL=1 after one decorrelation time)
- Causal information rates: dynamic causal relations
- Correlation between A(t) & B(t): $\Gamma(A,t) \sim \Gamma(B,t)$ even when $p(A,t) \neq p(B,t)$
- Quantify correlation, causality, hysteresis, forecast abrupt events & work better than entropy-based methods [E Kim, Entropy 23, 1393, 2021; Entropy 20, 574, 2018; Entropy 23, 1087, 2021]

Analytical expression for a Gaussian PDF

$$p(A,t) = \frac{1}{\sqrt{2\pi\sigma}} exp\left(-\frac{|A-\mu|^2}{2\sigma^2}\right)^2$$

$$\Gamma^2 = \left(\frac{dL}{dt}\right)^2 = \left(\frac{1}{\sigma}\frac{d\mu}{dt}\right)^2 + 2\left(\frac{1}{\sigma}\frac{d\sigma}{dt}\right)^2$$

So, a broad PDF with large σ gives smaller $\Gamma(t)$ and $L(t)$

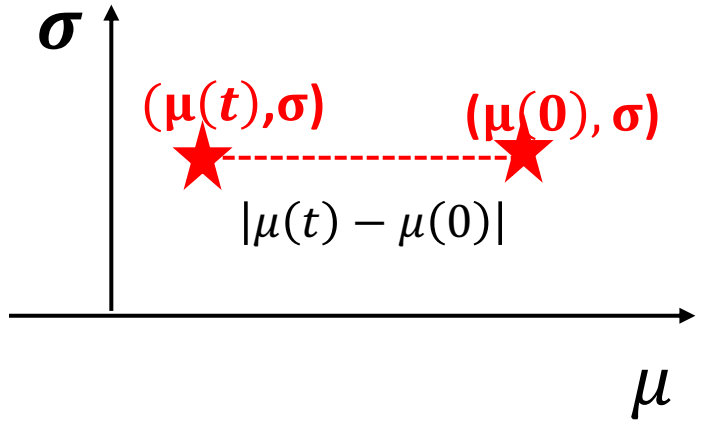

Poincare upper half-plane

For constant σ

$$\Gamma^2 = \left(\frac{dL}{dt}\right)^2 = \left(\frac{1}{\sigma}\frac{d\mu}{dt}\right)^2, \; L(t) = \frac{|\mu(t)-\mu(0)|}{\sigma}$$

$L(t)$ is quantized by σ (smallest distance that can be resolved)

Part IV – Information geometry of the L-H transition:

Stochastic prey-predator L-H transition model vs experimental data analysis

Information length in L-H-like transitions

Why it is useful

- Information length can reveal rapid statistical evolution before or during a transition
- It is sensitive to PDF-shape changes, not only to mean shifts
- In stochastic prey-predator models, it can quantify self-regulation between turbulence and zonal flows
- Potential use: regime identification and early-warning indicators

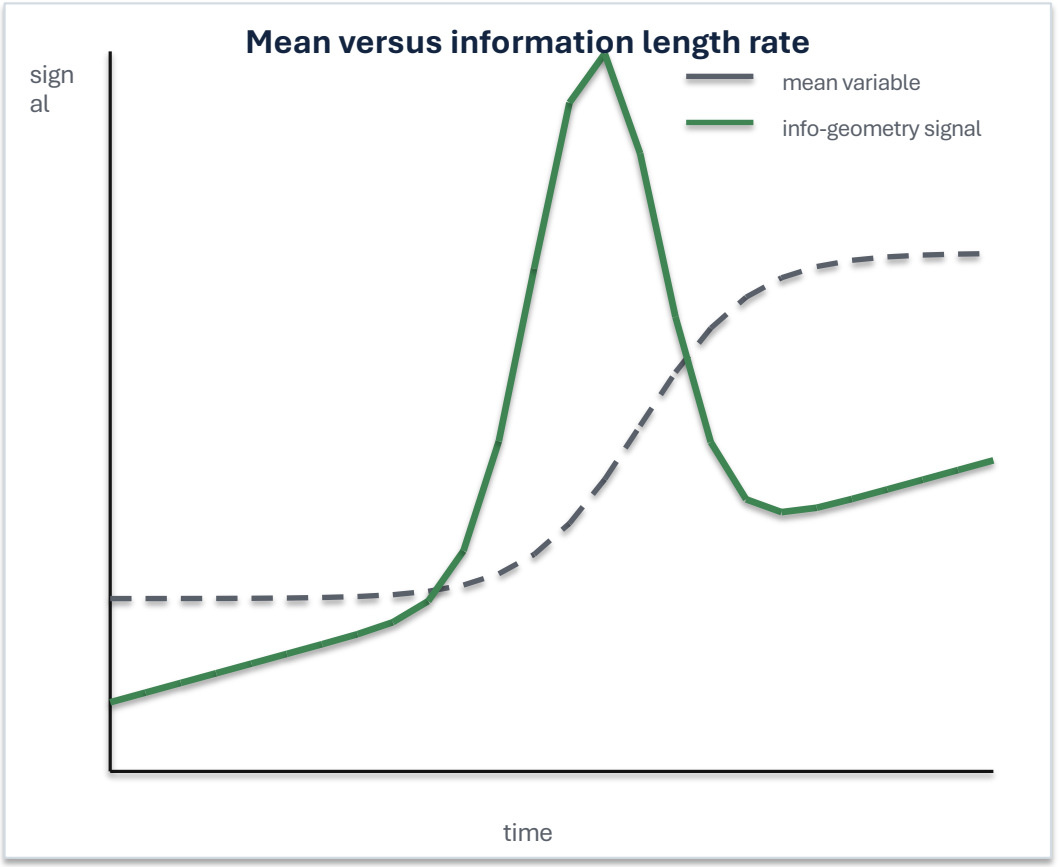

Revisit: Prey-predator stochastic L-H transition model

[E Kim et al, PPCF 2025; PRE 2024; Entropy 2024, P Fuller et al 2024, E Kim et al PRP 2020, R Hollerbach & Kim POP 2021]

$$\frac{d\epsilon}{dt} = N\epsilon - a_1\epsilon^2 - a_2V^2\epsilon - a_3v^2\epsilon + \xi_1\epsilon,$$

$$\frac{dv}{dt} = \frac{b_1\epsilon v}{1+b_2V^2} - b_3v + \xi_2,$$

$$\frac{dN}{dt} = -c_1\epsilon N - c_2N + Q + \xi_3.$$

- $\epsilon = x^2$: Turbulence amplitude (prey: rabbits)
- v: zonal flows (predator: foxes)
- N: Density (pressure) gradient
- Q: Input power (constant + fluctuation)
- V = dN^2: mean flow shear (super predator: lions)
- a_i, b_i, c_i, d: constant model parameters

- Based on E Kim & PH Diamond (PRL90, 185006, 2003): limit cycle oscillation (dithering) due to self-regulation between turbulence and self-generated zonal flows (also, see Malkov 2015, Hsu 2015, K Miki 2012)
  - Input power (heating) drives turbulence (prey) via instabilities
  - (Meso-scale) Zonal flow generated by turbulence regulate turbulence
  - (Macro-scale) Mean flow shears on larger scale (driven by density/pressure gradient) regulate both turbulence and zonal flow (super-predator, lions)

1. Sharp L-H transition: Information rate ($\Gamma^2 = \mathcal{E}$) forms a peak at the L-H transition (DIII-D experiments vs theory)

DIII-D
HJ Farre-Kaga et al 2023

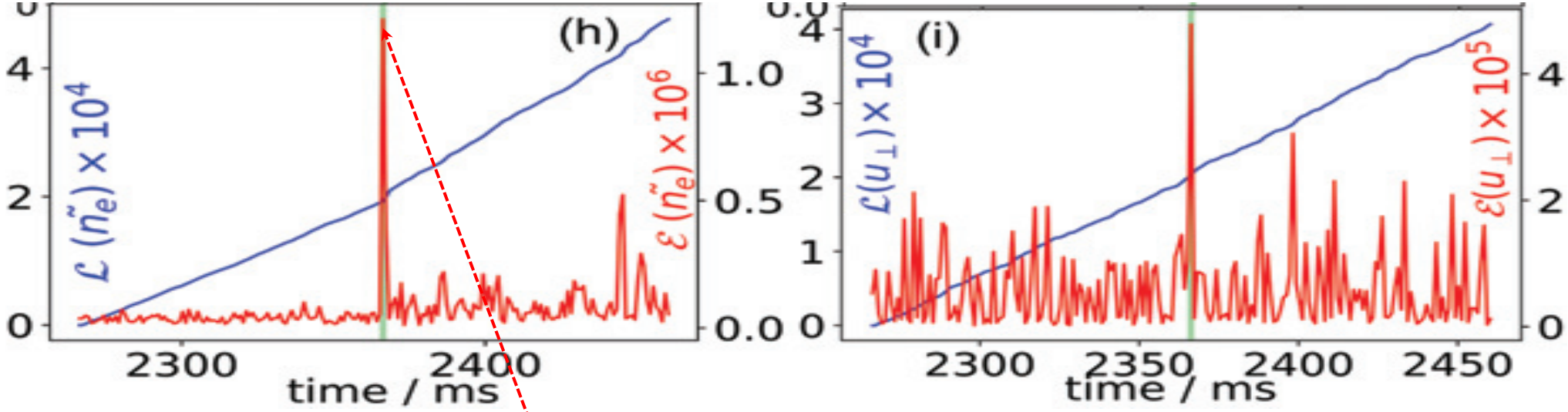

Prey-predator
E Kim 2024

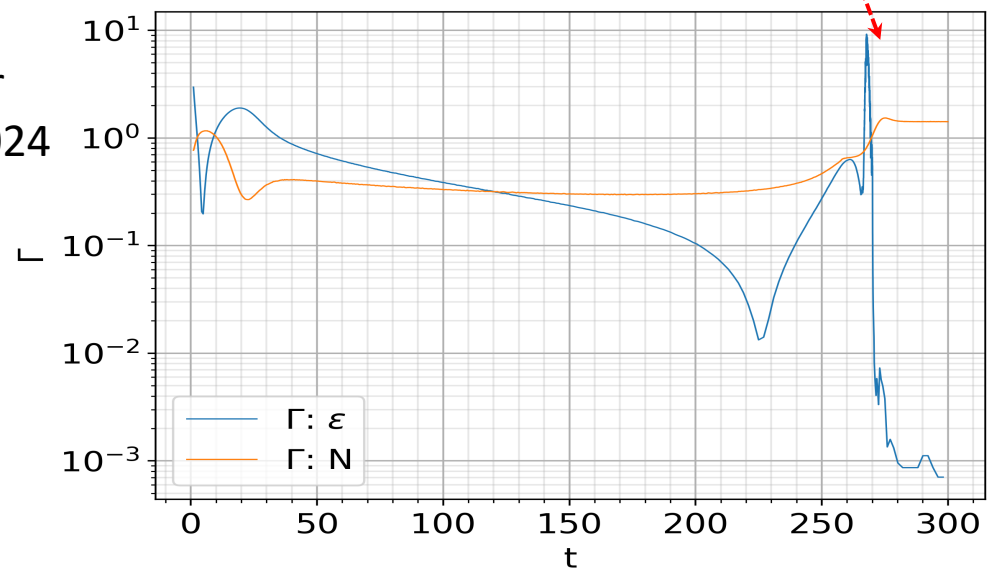

- Information rate (decorrelation rate) forms a spike at the L-H transition, similar to the model prediction without zonal flow.
- Information rate is larger in the H-mode

2. Dithering transition: Self-regulation captured by oscillatory information rates with phase shift between turbulence, zonal flows, and pressure gradient (E Kim et al 2024;2025)

$$\Gamma_\epsilon = 2\sqrt{\int d\epsilon \left[\frac{dq(\epsilon,t)}{dt}\right]^2},\ \Gamma_v = 2\sqrt{\int dv \left[\frac{dq(v,t)}{dt}\right]^2},\ \Gamma_N = 2\sqrt{\int \left[\frac{dq(N,t)}{dt}\right]^2}$$

(q=p$^{1/2}$)

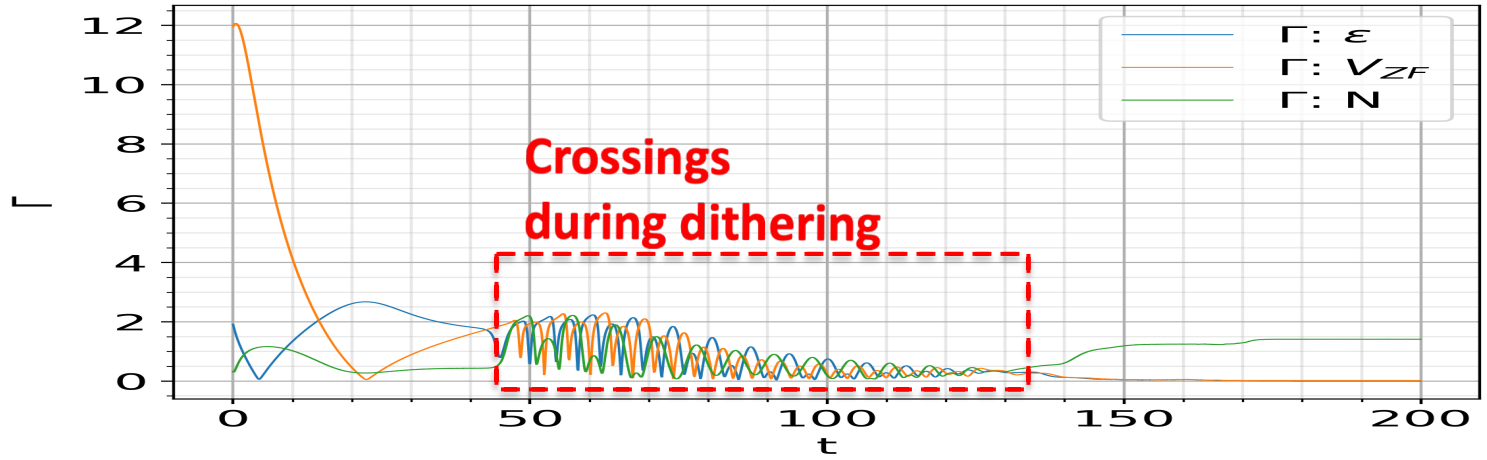

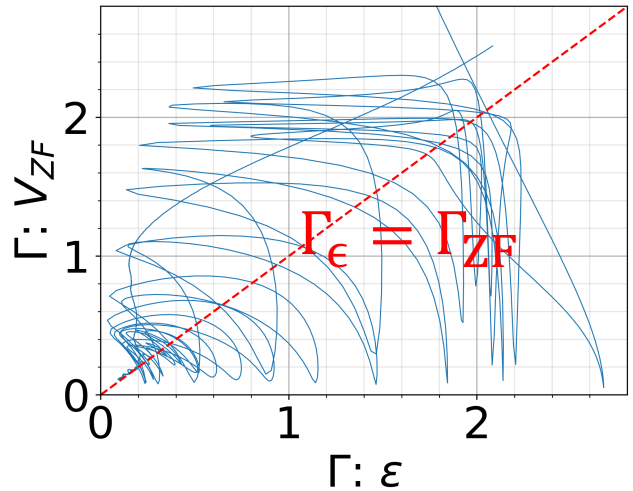

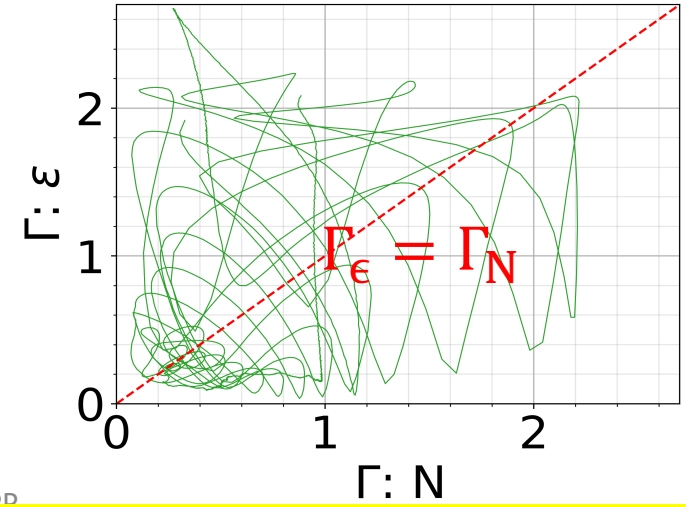

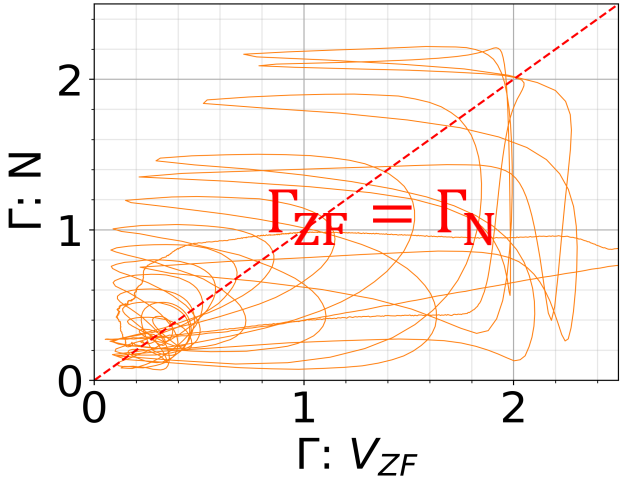

Self-regulation: crossing between Γ across a line with unit slope

Experimental support: Information rate oscillates with phase shift between fluctuations and u_{perp} (DIII-D: HJ Farre-Kaga et al 2023)

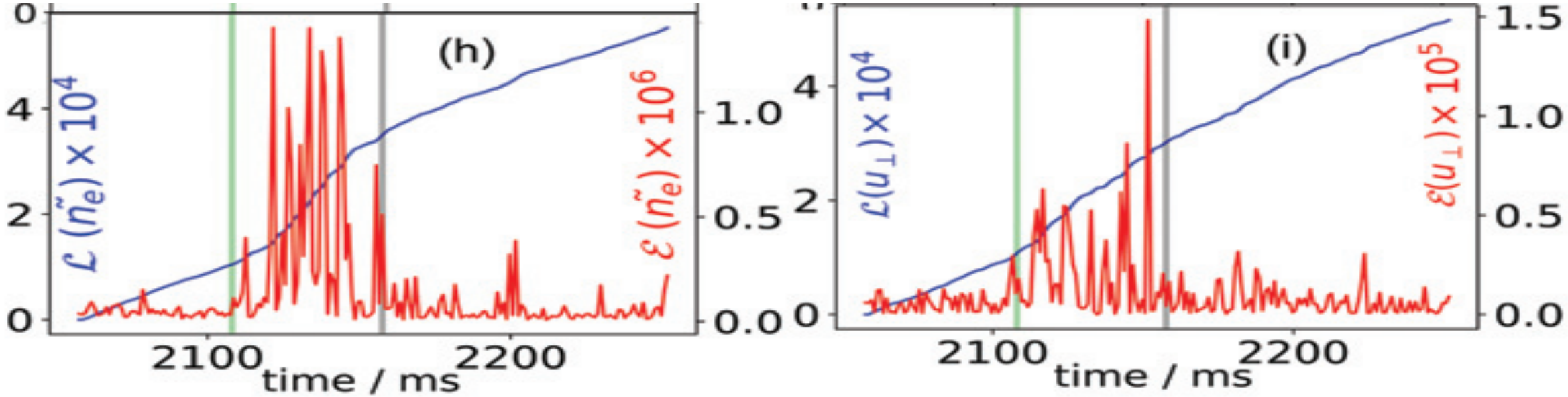

- During dithering, self-regulation is captured by oscillatory information rates of turbulence and u_{perp} with phase difference
- Information rate increases during dithering due to enhanced decorrelation rate
- $\Gamma \sim (2 \sim 5) \cdot 10^6$/sec (similar to ω_{EXB} , $\Delta\omega_D$ in Schmitz 2012)

T. Ashton-Key, Y. Andrew… E. Kim, et al (PPCF 2025)

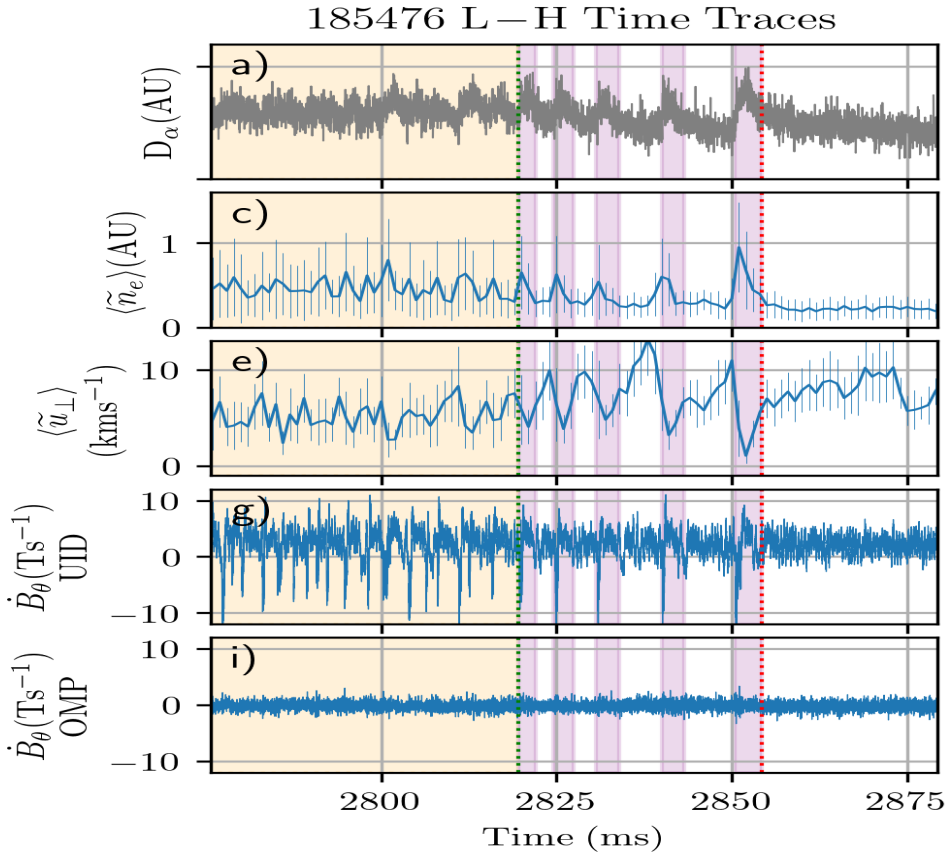

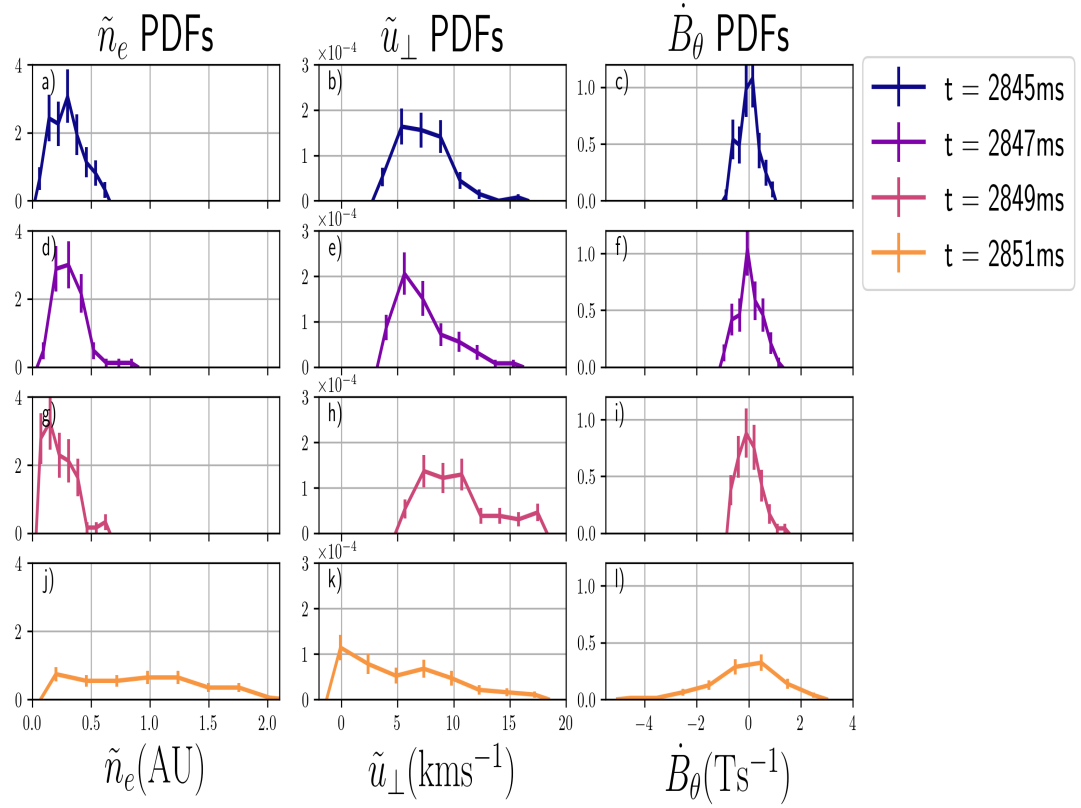

Self-regulation between turbulence and magnetic fluctuations from information geometry

- Information rate Γ against time
- n (density fluctuations)
- u (fluctuation perpendicular velocity)
- dBp/dt(magnetic fluctuations)

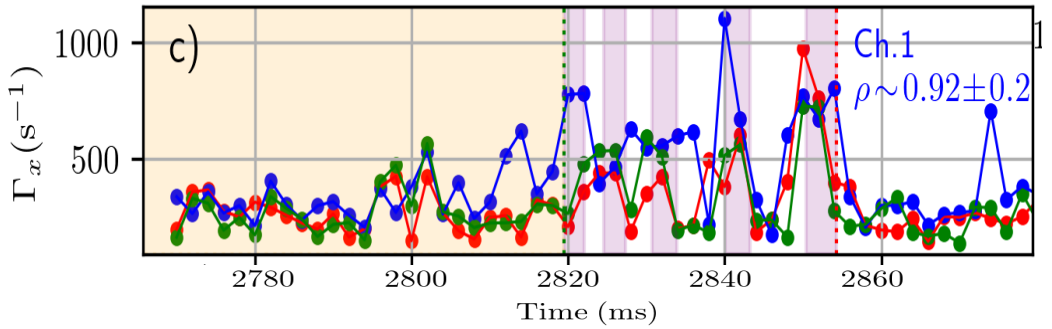

4. mHW: Similar information rates for fluctuations – correlations

Γ(ϕ), Γ(n), Γ(ω) for total; Γ($\tilde{\phi}$), Γ($\tilde{n}$), Γ($\tilde{\omega}$) for fluctuations; Γ(⟨ϕ⟩), Γ(⟨n⟩), Γ(⟨ω⟩) for zonal flows

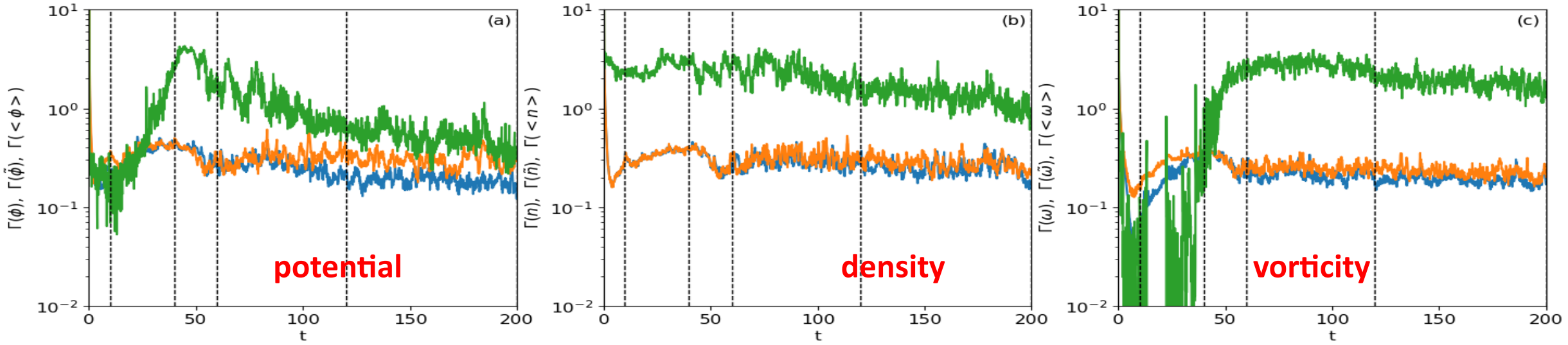

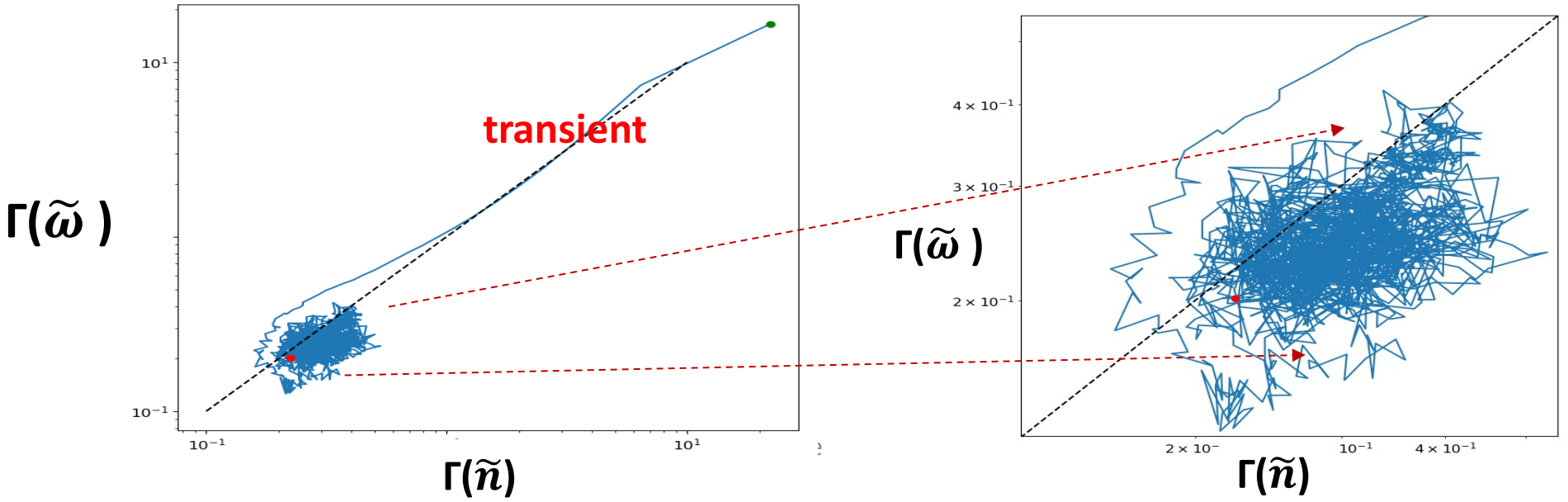

3. Self-organization is manifested by an almost constant information rate of joint PDF [P Fuller, E Kim, et al, PoP 31, 092506, 2024]

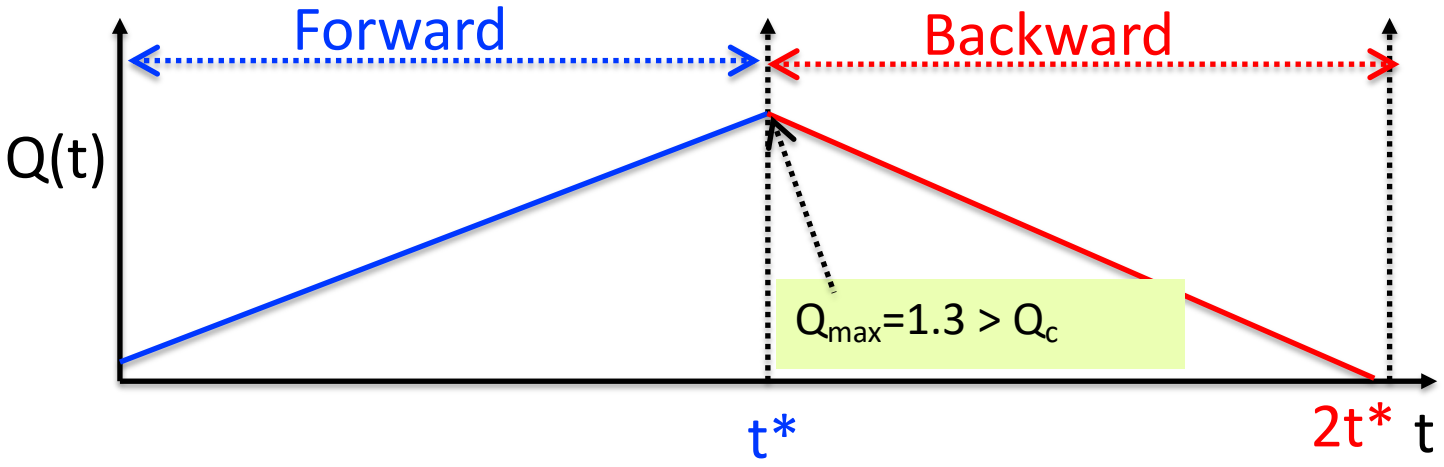

$$\Gamma(t) = \left[\int dx\, dv\, dN \frac{1}{p(x,v,N,t)} \left[\frac{\partial p(x,v,N,t)}{\partial t}\right]^2\right]^{1/2}$$

$$\Gamma_v(t) = \left[\int dv \frac{1}{p_v(v,t)} \left[\frac{\partial p_v(v,t)}{\partial t}\right]^2\right]^{1/2}$$

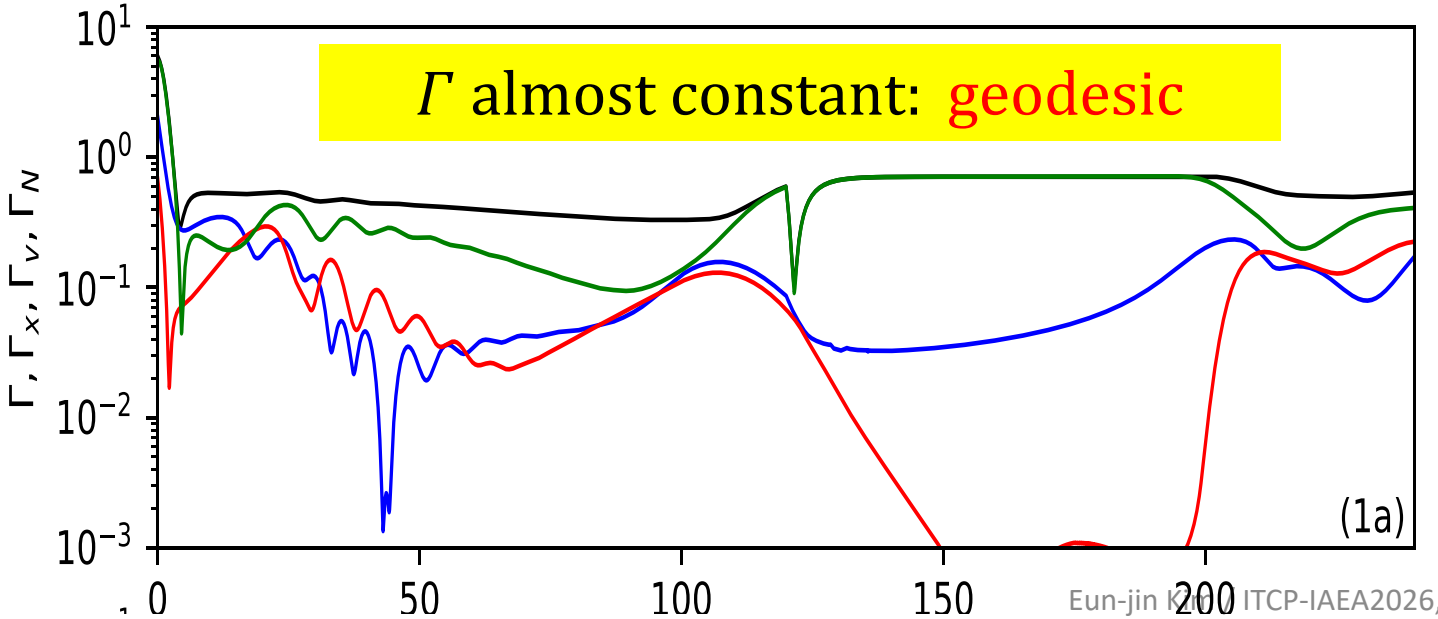

- Joint PDF: Γ in black
- Marginal PDFs: Γ_v in red, Γ_N in green, Γ_x in blue

- Self-organization = geodesic? (E Kim PRE 95, 062107, 2017)

5. Effects of dynamical change in statistical state of one variable on that of another variable

Causal information rate (E Kim, Entropy 23, 1087, 2021; PRE 2024)

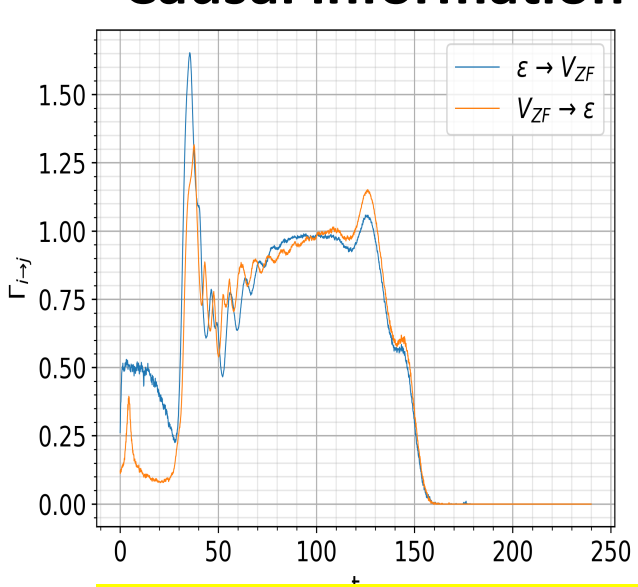

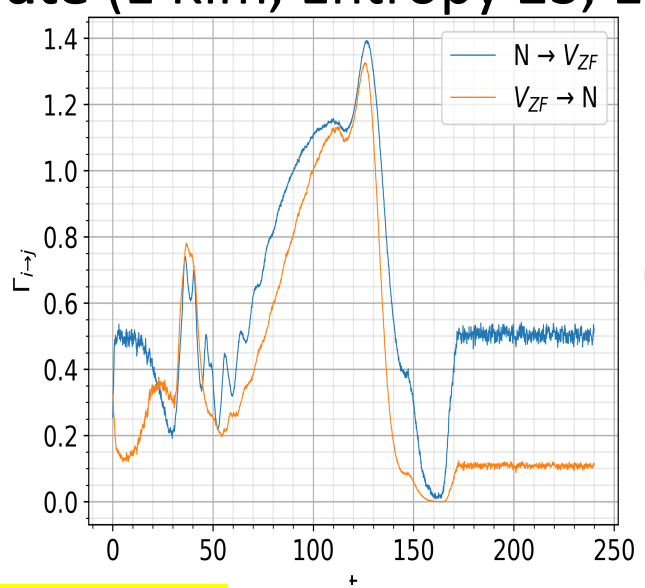

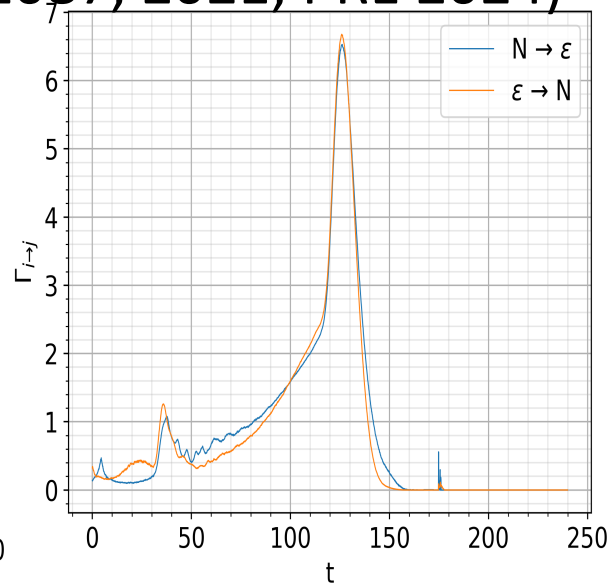

cf: Instantaneous Transfer entropy

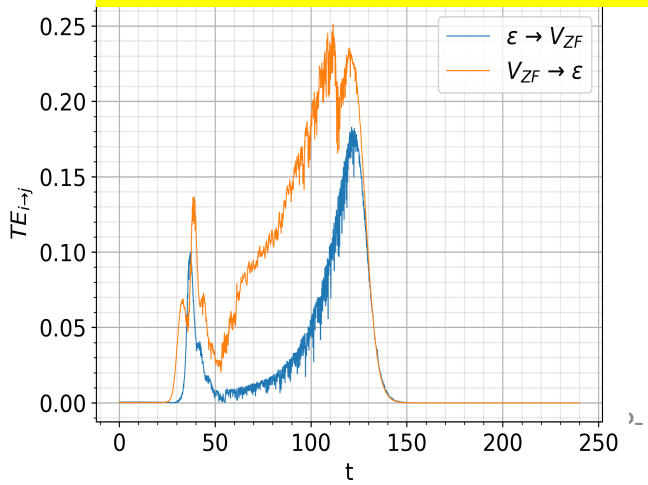

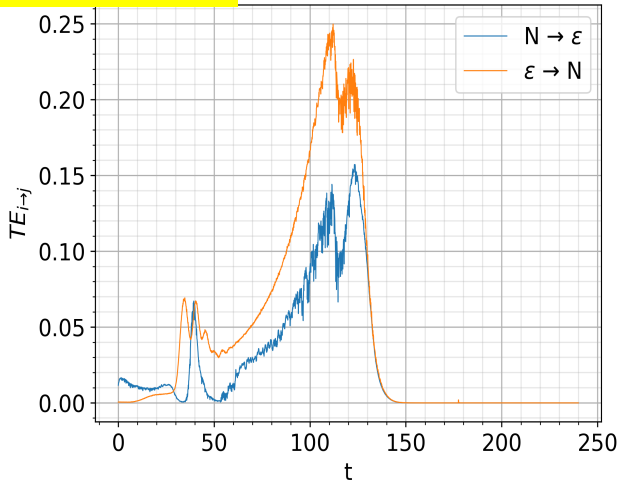

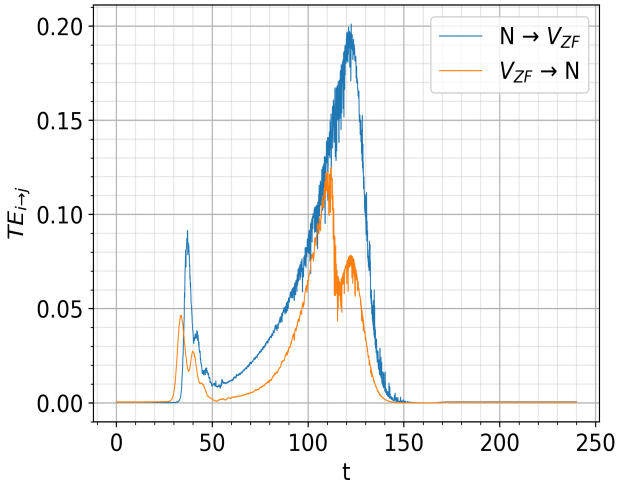

Net causal information rates and net causality $\Gamma_{\epsilon\to v} - \Gamma_{v\to\epsilon}$ etc. reveal the sequence of events over the L-H transition

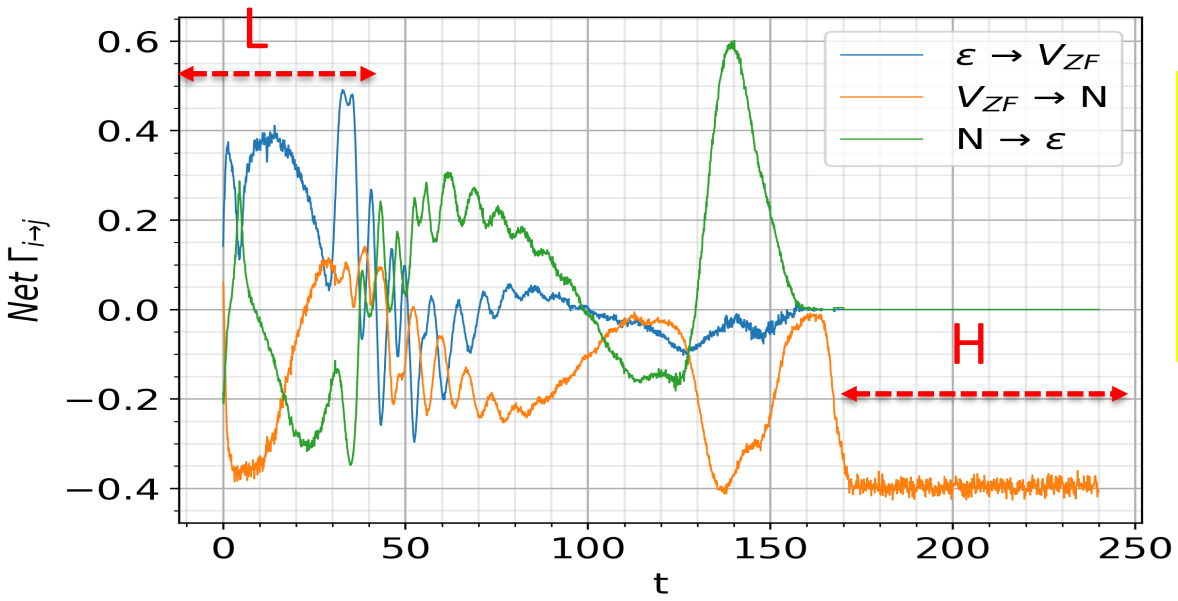

cf. Net transfer entropy

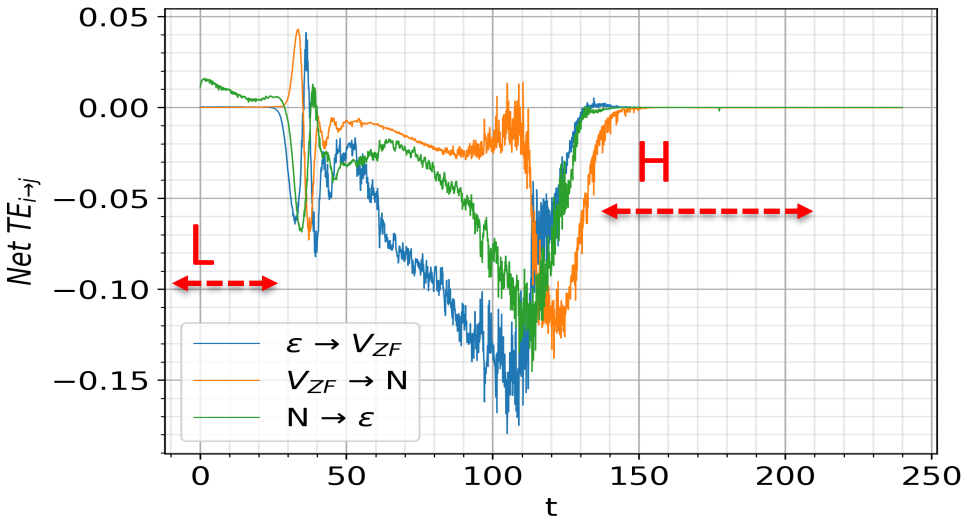

L-mode: $\mathbf{N} \to \boldsymbol{\epsilon}, \boldsymbol{\epsilon} \to \boldsymbol{v}, \boldsymbol{N} \to \boldsymbol{v}$

Dithering: $\boldsymbol{\epsilon} \leftrightarrow \mathbf{v}$ **(self-regulation),** $\boldsymbol{N} \to \boldsymbol{v}$

H-mode: $\mathbf{v} \to \boldsymbol{\epsilon}$, $\mathbf{N} \to \boldsymbol{\epsilon}, \boldsymbol{N} \to \boldsymbol{v}$

Dithering:

$\mathbf{v} \to \boldsymbol{\epsilon}$ **(not reflect self-regulation)**

Part VI – Summary, Open problems

Summary

- Turbulence statistics are not only spectra; PDFs, tails, dependencies and trajectories in probability space matter
- Non-perturbative methods target coherent structures and rare events that perturbative closures can miss
- Information theory quantifies nonlinear dependence and directed influence, but causality needs careful assumptions
- Information geometry provides a useful tool to understand time-dependent PDFs and transitions

Multiscale fusion turbulence

The pedestal and edge are not single-scale problems

Open problem

Ion-scale turbulence alone often fails to explain observed transport.

Electron-scale turbulence and cross-scale coupling can change saturation and transport.

Pedestal transport may involve ETG, MTM, ITG/TEM, KBM/MHD-like physics in different channels.

Scale hierarchy and channel coupling

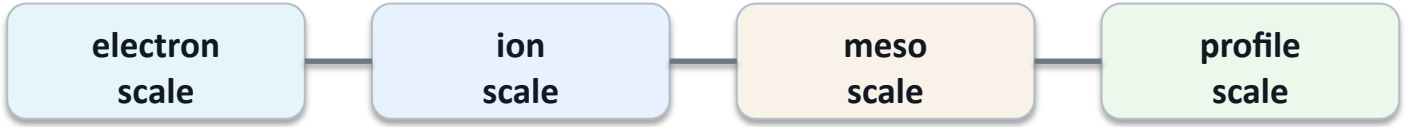

ETG / MTM can set electron heat flux while zonal flows, avalanches, and profiles regulate saturation.

Fingerprint idea

Identify dominant modes from ratios of Qe, Qi, Γe, impurity flux, and fluctuation frequency.

Needed next

Coupled gyrokinetics + synthetic diagnostics + probabilistic modelling + experiments.

Refs: Maeyama et al., Nucl. Fusion 64, 112007 (2024); Kotschenreuther et al., Nucl. Fusion 59, 096001 (2019); Hatch et al., Nucl. Fusion 56, 104003 (2016).

Further reading

- Biglari, Diamond & Terry, Phys. Fluids B 2, 1 (1990).
- Hahm & Burrell, Phys. Plasmas 2, 1648 (1995).
- Burrell, Phys. Plasmas 4, 1499 (1997).
- Diamond et al., Plasma Phys. Control. Fusion 47, R35 (2005).
- Wagner, Plasma Phys. Control. Fusion 49, B1 (2007).
- Kim & Anderson, Phys. Plasmas 15, 114506 (2008).
- Kim & Hollerbach, Phys. Rev. Research 2, 023077 (2020).
- Eich et al., Nucl. Fusion 53, 093031 (2013).
- E Kim, Phys. Plasmas 32, 070902 (2025).
- E Kim, Entropy 23, 1393, 2021; Entropy 20, 574, 2018.
- E Kim, Entropy 23, 1087, 2021
- E Kim & PH Diamond, PRL 90, 185006, 2003
- E Kim & R Hollerbach, Phys Rev Research 2, 023077, 2020
- R Hollerbach, E Kim & L Schmitz, PoP 27, 202301, 2020
- HJ Farre-Kaga, Y Andrew, J Dunsmore, E Kim, TL Rhodes, L Schmitz, Z Yan, Europhysics Letters 142,64001, 2023
- Y Andrew, J Dunsmore, T Ashton-Key, H Farre Kaga, E Kim, et al, Plasma Phys. Control. Fusion 66, 055009, 2024
- E Kim & A Thiruthumal, Entropy 26, 17, 2024
- P Fuller, E Kim, et al, PoP 30, 102502, 2023
- J Anderson, E Kim, B Hnat et al, PoP 27, 022307, 2020
- A Papadopoulos, J Anderson, E Kim et al, Entropy 25, 942, 2023

References are compact lecture pointers; consult the papers for model assumptions and quantitative regimes.